TALLINNA TEHNIKAÜLIKOOL
TALLINN UNIVERSITY OF TECHNOLOGY

DEPARTMENT OF MATERIALS AND
ENVIRONMENTAL TECHNOLOGY

SPRAY DEPOSITED ALUMINUM OXIDE THIN FILMS FOR ELECTRONIC APPLICATIONS

PIHUSTUSPÜROLÜÜSI MEETODIL SADESTATUD ALUMIINIUMOKSIIDI ÕHUKESED KILED ELEKTROONIKASEADISTELE

MASTER THESIS

Student: ……..Khalil Dolapo Omotosho.....
/name/
Student code: ……..173969KAYM.....
Supervisor: Abayomi Oluwabi, Early Stage Researcher;
……Ilona Oja Acik, Senior Researcher…..
/name, position/

Tallinn, 2019

AUTHOR'S DECLARATION

I hereby declare, that I have written this thesis independently.

No academic degree has been applied for based on this material. All works, major viewpoints and data of the other authors used in this thesis have been referenced.

".....” ……..201.....

Author: ……

/signature /

Thesis is in accordance with terms and requirements

".....” ……..201……

Supervisor: ……..

/signature/

Accepted for defence

".....” .....201…..

Chairman of theses defence commission: .....

/name and signature/

Department of Materials and Environmental Technology

THESIS TASK

Student: Khalil Dolapo Omotosho, 173969KAYM

Study programme: KAYM09/09 Materials and Processes for Sustainable Energetics

Main speciality: Processes for sustainable energetics

Supervisors: Early stage researcher, Abayomi Oluwabi, +37253912622; Senior research scientist, Ilona Oja ACik, +3726203369...

Thesis topic:

(in English) *Spray deposited aluminum oxide thin films for electronic applications*
(in Estonian) *Pihustuspürolüüsi meetodil sadestatud alumiiniumoksiidi õhukesed kiled elektroonikaseadistele*

Thesis main objectives:

1. To deposit AlO_x thin films by chemical spray pyrolysis at various deposition temperatures.
2. To Investigate surface morphology and structural characteristics of AlO_x thin films.
3. To analyse the electrical properties of the deposited AlO_x thin films.

Thesis tasks and time schedule:

No	Task description	Deadline
1.	To deposit AlO_x thin films on Si and quartz substrates at different deposition temperatures and anneal at different temperatures.	19.10.2018
2.	To analyse the surface morphology, structural, and electrical properties of AlO_x thin films.	12.02.2019
3.	To write the master thesis	27.05.2019

Language: …English… **Deadline for submission of thesis:** "...27...." .....May.....2019

Student: Khalil Dolapo Omotosho ..... "....."....201…a
/signature/

Supervisor: Abayomi Oluwabi ..... "....."....201…a
/signature/

TABLE OF CONTENTS

PREFACE

The project before you is titled “spray deposited aluminum oxide thin films for electronic applications”. This project involves deposition of aluminum oxide thin films by the ultrasonic spray pyrolysis method and characterizing it to determine its suitability for application as a dielectric layer. This thesis has been conscientiously written to fulfil the graduation requirements of the Masters of Science Degree in Materials and Processes for Sustainable Energetics Programme at Tallinn University of Technology, Estonia**.**

This work is financially supported by the Estonian Ministry of Education and Research projects IUT 19-4 and by the European Union through the European Regional Development Fund “Centre of Excellence” project TK141: Advanced materials and high technology devices for sustainable energetics, sensorics and nanoelectronics.

Firstly, I give glory to almighty Allah for seeing me through this programme. My deepest appreciation goes to my supervisor, Abayomi Oluwabi, Phd student at the department of Materials and Environmental Technology for his guidance and suggestions in carrying out experiments and measurements, for everything he taught me also for his criticisms which have been helpful towards the completion of this thesis. I also would like to appreciate the efforts and contributions of my co-supervisor, Dr. Ilona Oja Acik, head of the Laboratory of Chemical Thin film Technologies who gave me this interesting topic. Also, my sincere gratitude to Dr. Valdek Mikli for the SEM measurements, and all members of the Laboratory of Chemical Thin film Technology for always coming to my aid whenever I needed assistance.

I would like to sincerely thank everyone who has supported me in one way or the other during this programme and made life easy for me in Estonia. My profound gratitude to my parents, Barr. and Mrs. Omotosho, my brothers, Habib and Muhammad, and my friends for their unwavering supports. I couldn’t have done this without them.

Finally, I would like to express my sincere gratitude to the Estonian government and Tallinn University of technology for supporting my studies and research through the tuition waiver scholarship, speciality scholarship, performance scholarship, dora scholarship and need based scholarships. I also want to thank KAYM program coordinator, Dr. Sergei Bereznev for his administrative role and support throughout the phase of this project.

Khalil Dolapo Omotosho

List of abbreviations and symbols

AlO_x – Aluminum oxide

CVD – Chemical vapor deposition

CSP – Chemical spray pyrolysis

CdS – Cadmium Sulphide

DNA – Deoxyribonucleic acid

EDX – Energy dispersive x-ray spectroscopy

FET – Field effect transistor

HfO_2 – Hafnium oxide

ISI – Institute for scientific information

ITO – Indium tin oxide

JVST – Journal of vacuum science and technology

MOS – Metal-oxide semiconductor

MOSFET – Metal-oxide semiconductor field effect transistor

OMVPE – Organometallic vapor phase epitaxy

PEALD - Plasma enhanced atomic layer deposition

PECVD – Plasma enhanced chemical vapor deposition

P3HT – Poly(3-hexylthiophene 2,5-diyl)

Ref - Reference

RMS – Root mean square

RT – Room temperature

SEM – Scanning electron microscopy

Sb_2S_3 – Antimony sulphide

Sn_xS_y – Tin sulphide

TFT- Thin film transistor

T_{an} - Annealing temperature

T_s – Substrate temperature

TiO_2 – Titanium (IV) oxide

UHV – Ultra-high vacuum

VPE – Vapor phase epitaxy

XPS – X-ray photoelectron spectroscopy

Y_2O_3 – Ytrrium oxide

ZrO_2 – Zirconium oxide.

TMA - Trimethylaluminum

1.0 INTRODUCTION

Oxide materials are promising for industrial production and sustainable development due to their abundance on earth, low cost and environmental friendly features as well as easy processing [1]. Beneficial properties offered by new families of materials like the metal oxides and organic semiconductors have prompted a shift in research for thin film transistor (TFT) from amorphous silicon to new semiconductor materials [2]. Materials with high dielectrics such as ZrO_2, Y_2O_3, HfO_2, AlO_x have been investigated and they are promising. However, aluminum oxide (AlO_x) is unique among other materials because of its abundance in nature, low cost, good chemical stability, high breakdown field, and low interfacial trap density with oxide semiconductors. Other properties of AlO_x that make it suitable for use as a dielectric material in TFT are; wide band gap (9.9 eV), high dielectric constant, low leakage current densities, and good adhesion to glass substrate [3]–[5].

Amorphous AlO_x is considered a suitable gate dielectric in TFTs because of its high permittivity value, and wide band gap which helps to avoid leakage current through crystalline grain boundaries [4]. In order to reduce the size of metal oxide semiconductor (MOS) transistors below 50 nm for next generation electronic devices, amorphous materials that are novel with high dielectric constant, high breakdown voltage, low leakage current and low interface trap density values are needed [5]. AlO_x has a band gap and dielectric constant of 9.9 eV and 10 respectively compared to SiO_2 with band gap of 9 eV and dielectric constant of 3.9 [5].

According to the literature review, several deposition methods have been employed to deposit thin films of aluminum oxide. Examples of such methods are sol-gel based method [6]–[8], Chemical Spray Pyrolysis (CSP) [9], [10], Chemical Vapor Deposition (CVD) [11], [12], Pulsed laser deposition [5], Plasma Enhanced Atomic Layer Deposition (PEALD) [13], Filtered Cathodic Vacuum Arc [14], Plasma Enhanced Chemical Vapor Deposition (PECVD) [15], Vacuum Evaporation [16]. CSP has been adopted as the deposition method for the purpose of this thesis because it's an easy and inexpensive technique for depositing thin films on large substrate area [17]. CSP offers ease in doping films with virtually any element by mixing the solutions in any proportion and adding it to the spray solution, it does not depend on high quality substrates and/or targets, no vacuum is needed, and both the deposition parameters and film thickness can be changed with ease [18].

This thesis is aimed at studying the electrical properties of CSP deposited Aluminum oxide thin films which could be used as a gate dielectric material in TFT. The influence of varying film deposition temperature and the effect of post deposition annealing temperature on the thin film properties

are presented. The deposited AlO_x thin films were characterized to study their structural, morphological, and electrical properties.

In chapter one, the thesis was introduced by stating the background and specific objectives of the research study.

Literatures on various research carried out on AlO_x thin films were reviewed in chapter two. Chapter two also discusses the various structures of AlO_x and their applications, different methods of deposition of AlO_x thin films, importance of the CSP method, applications of AlO_x thin films, and finally overview of thin film transistor and its structures.

Chapter three contains materials and methods used to carry out experimental work, and experimental procedures, including detailed discussion of the apparatus and reagents used. It further reviews the characterization techniques and the instruments used to achieve that.

Chapter four presents the results of the experiments carried out, detailed discussions and analysis of results and some valid recommendations for future research. Chapter five elucidates a detailed summary of all the work done.

2.0 LITERATURE REVIEW

2.1 Aluminum oxide (AlO_x)

AlO_x is a very important insulating material due to its high dielectric break-down field, wide bandgap, and a high dielectric constant [19]. It is also a multipurpose and technologically significant material because of its transparency over a wide range of wave length from ultra-violet to mid-infrared, good thermal and chemical stability, and superior electrical and mechanical properties [7].

AlO_x occur in numerous crystallographic polymorphs [20]. More than 45 million tons of AlO_x produced in the world are manufactured industrially majorly by the Bayer method using bauxite, and about 40 million tons are utilized for refining aluminum.

Around 5 million tons of AlO_x are manufactured as chemical grade and employed for several functions. Furthermore, approximately 1.5 million tons of AlO_x is served as raw powder in the world, and the remainder is used for raw powder of aluminum hydroxide, aluminum sulfate and polyaluminum chloride [21].

AlO_x exists in different forms of crystalline structure such as α (trigonal), θ (monoclinic), γ, η (cubic), δ (either tetragonal or orthorhombic) and these structures represent the important crystalline phases in the alumina structure[22]. The crystal structure of aluminum oxide can be seen in Figure 2.1. α-AlO_x is the most stable type of the compounds formed between aluminum and oxygen at high temperature with melting temperature of 2051 ^{o}C [23], and is the final product from thermal or dehydroxylation treatments of all the hydroxides [21].

As seen in Table 2.1, α-AlO_x also has a high density of 3980 Kg/m^3, high elastic modulus of 409 Gpa, and a high hardness of 28 Gpa. These properties show that α-AlO_x has excellent physical and mechanical properties compared to γ and θ alumina phases. Figure 2.2 shows that the α-phase alumina does not change to γ and θ phases, while the γ and θ phases transform to the corundrum phase at specific temperature [23].

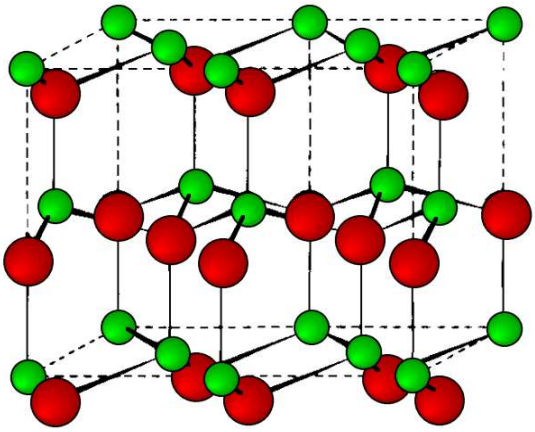

Figure 2.1 Crystal structure of alumina [79]

Table 2.1 Mechanical and physical properties of alumina phases at different melting temperatures [23]

Alumina	**Selected Properties**			
	Density, kg/m^3	**Elastic Modulus, Gpa**	**Hardness, Gpa**	**Melting Temperature, °C**
α-Alumina	3980	409	28	2051
γ-Alumina	3200	-	-	$\gamma \rightarrow \delta$: 700-800
θ-Alumina	3560	-	-	$\theta \rightarrow \alpha$: 1050

Other forms are commonly called transition AlO_x and they appear during the thermal decomposition of aluminum trihydroxides under dissimilar conditions [21].

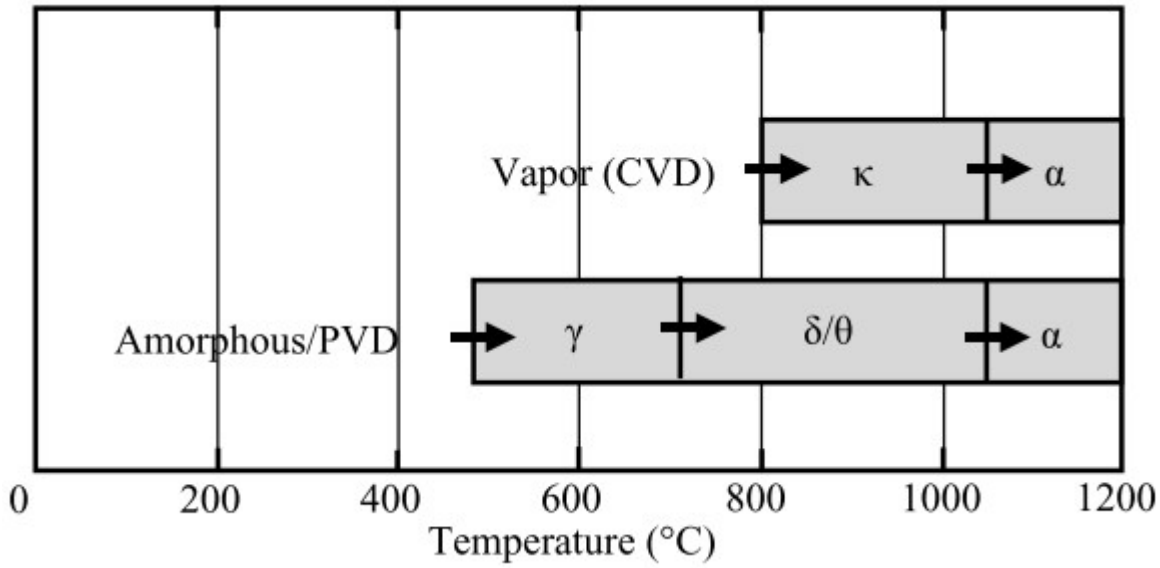

Figure 2.2 Transition stages of alumina phases at different temperatures [23]

Θ-phase Alumina is one of the unstable phases of Alumina which is transformed into the α-phase at temperature of about 1050 °C. Θ-phase has a lower density of about 3560 kg/m^3 compared to a density of 3980 kg/m^3 for α-phase [23]. Sequence of phase transformations of alumina may be influenced by factors such as particle size, heating rate, impurities and atmosphere as a result of their effect on the kinetics of transformation [24]. The γ-alumina phase is an unstable phase that has been used as a catalyst and catalyst support due to its large specific area and low surface energy. It is transformed to Θ-alumina phase at a temperature of 700-800 °C. The lattice structure for γ-alumina phase has two different lattices consisting of Aluminum ions which is formed from octahedral and tetrahedral interstitial locations and oxygen lattice formed with the face-centered cubic structure [23].

Single crystal α-alumina phase is called sapphire. It crystallizes in the corundum structure to form sapphire mono crystals. Polycrystalline α-alumina is suitable as a structural ceramic due to its good mechanical properties, high strength and excellent thermal properties at high temperature. It acquires these properties during developing, processing, and optimizing the polycrystalline alumina [23]. Polycrystalline α-alumina also has a high chemical stability and heat resistance which makes it suitable to fabricate high pressure sodium lamps from translucent alumina [23].

Table 2.2 Applications and properties of high purity grade alumina [23]

Grade	**Al_2O_3 Content, %**	**Kind of product and applications**	**Porosity %**	**Density g/cm^3**	**Applications**
A1	>99.6	Electrical and Engineering	0.2-3	3.75-3.95	Structural
A2	>99.8	Translucent	<1	3.90-3.99	Sodium lamp
A3	>99.5	Hot-pressed	<1	3.80-3.99	Machine tools
A4	>99.6	Sintered recrystallised	3-6	3.75-3.85	Refractory
A5	99.0 – 99.6	Low dielectric	1-5	3.76-3.94	Microwave

Table 2.3 Applications and properties of low purity grade alumina [23]

Grade	**Al_2O_3 Content, %**	**Kind of product and applications**	**Porosity %**	**Density g/cm^3**	**Applications**
A6	99.5-99.0	Electrical and Engineering	1-5	3.71-3.92	Mechanical and Electrical
A7	94.5-96.5	Electrical and Engineering	2-5	3.60-3.90	Insulators and Wear parts

Grade	Al_2O_3 Content, %	Kind of product and applications	Porosity %	Density g/cm^3	Applications
A8	86.0-94.5	Electrical and Engineering	2-5	3.40-3.90	Insulator, Wear parts, Refractory
A9	80.0-86.0	Electrical and Engineering	3-6	3.30-3.60	Insulator, Wear parts, Refractory

Polycrystalline alumina is divided into 2 sets, depending on the alumina purity and applications. These are the high purity alumina and low purity alumina. High purity alumina properties with purity of at least 99% alumina can be seen in Table 2.2. Low purity alumina with purity of 80% to 99% alumina which represents the second group is shown in Table 2.3.

Table 2.4 presents the thermal properties of high purity grade alumina and low purity grade alumina in terms of thermal expansion coefficient, specific heat, enthalpy and the thermal conductivity properties. High purity grade alumina have high thermal conductivity in the range of 25 – 40 W/m.K, while the low purity grade alumina have thermal conductivity in the range of 15 – 30 W/m.K.

Table 2.4 Thermal properties of higher and lower purity alumina at 25^{o}C [23]

Grade	Thermal Expansion Coefficient 10^{-6} (1/K)	Specific Heat (J/g.K)	Enthalpy at 25 ^{o}C, (J/g)	Thermal Conductivity (W/m.K)
A1	5.4	0.775	0	30 - 40
A2	5.4	0.775	0	30 - 40
A3	5.4	0.775	0	27 - 40
A4	5.4	0.775	0	25 - 35
A5	5.4	0.780	0	30 - 40
A6	5.1 - 5.4	0.780	0	25 - 30
A7	5.1 - 5.4	0.760 - 0.780	0	20 - 30
A8	4.9 - 5.5	0.755 - 0.785	0	15 - 20
A9	4.9 - 5.5	0.750 - 0.785	0	15 - 20

AlO_x can be processed into different forms such as thick and thin films, porous films, nanocrystalline, and polycrystalline particles, among many others. Nanoparticles of AlO_x have been studied and characterized by Vijaya Dhawale et al. [25] and Ravindhranath et al. [26] for water treatment of colored industrial effluents and the removal of toxic ions from water due to their large surface area, high surface energies and potentials, and availability of surface functional groups for binding over

the pollutants. Nina Doskocz et al. [27] investigated the effect of AlO_x nanoparticles on bacterial growth, and they reported that nanoparticles of AlO_x impede the growth of P. putida bacterial and it has a higher impact on the bacterial than macro-form of AlO_x when they are in comparison.

A review on the application of nanoparticles of AlO_x in the biomedical industry have been carried out by Peyman et al. [28]. They reported that nanoparticles of AlO_x are applied in biomedicine; as a drug delivery vehicle, in biosensing of different molecules like DNA in a competitive bioassay, in cancer therapy, as anti-microbial growth, in treatment of diseases like asthma, in stabilization and preservation of biomolecules like protein to prevent aggregation and mis-folding, in immunotherapy and next generation vaccines.

AlO_x is a valuable material in contemporary materials technology in comparison with other ceramic materials [21]. Due to its high dielectric constant (approx. 10), high thermal stability (up to 1000 ^oC), high band gap (9.9 eV) and high insulative properties, aluminum oxide is a very promising material in optoelectronics and microelectronics devices [5], [29]. As a result of its stability as an insulator and higher radiation resistance than SiO_2, Aluminum oxide has several advantages over SiO_2 for semiconductor applications [30].

Nanostructured Aluminum oxide is used as a passivation layer in solar cells, as a dielectric material in MOSFET, for water purification [31], firebricks, integrated circuit, abrasives, anti-reflection coating, sensors, gas diffusion barrier, biomedicine and neurosurgery [21], [32], [33].

Thin films of AlO_x which is the focus of this study have been studied extensively using several deposition methods for different applications in microelectronics, optoelectronics [5], [6], [34]–[39], and photovoltaics [40] industry and for corrosion protection [41][42].

2.2 AlO_x thin films

AlO_x thin films are grown via physical/chemical deposition methods such as; electron beam evaporation, pulsed laser deposition, sputtering, chemical vapour deposition, metal-organic chemical vapour deposition, and plasma-enhanced chemical vapour deposition [13].

AlO_x thin films are useful as dielectric layers on several types of microelectronic devices [10], as an anti-reflection coating and passivation film for silicon-based solar cells [40], biomedicine, neurosurgery, and optoelectronics [32].

Che-Chu Lin et al. [40] demonstrated that Liquid phase deposition AlO_x thin film is favorable for use as antireflection and passivation properties for silicon nanowire based solar cells. P. Katiyar et al. [5] also reported that AlO_x thin films prepared using pulsed laser deposition method are suitable for high dielectric constant materials in next generation electronic devices.

2.3 AlO_x thin film deposition methods

Physical deposition method involves the transportation of atoms /molecules of the materials to be deposited from a source to the substrates where they bond to form a film using mechanical, electromechanical or thermodynamic processes [48]. It is divided majorly into vacuum evaporation and sputtering. Vacuum evaporation operates at a low background pressure, while sputtering involves the release of atoms or molecules from the surface of a material target by a mechanism of momentum transfer resulting from an impact from ionized inert gas atoms [49].The physical methods include; physical vapour deposition (PVD), laser ablation, molecular beam epitaxy, and sputtering [17]. The major advantage of this deposition method is that they produce good quality film. However, they are highly expensive and they require large amount of material target [50].

On the other hand, the chemical deposition method employs a fluid precursor which decompose on the substrate to produce a thin film. It is divided into gas-phase deposition methods and solution techniques. The gas-phase method is further divided into chemical vapour deposition (CVD) and atomic layer epitaxy (ALE). While the solution technique method comprises of spray pyrolysis, sol-gel, spin and dip-coating [17]. The chemical deposition technique relies heavily on the chemistry of solutions, pH value, and viscosity [50]. They produce good quality films, and they are economical to use as they mostly do not require expensive equipments [50].

According to the ISI web of science database, different methods of deposition that have been used to deposit AlO_x films with their number of publications are presented in Figure 2.3

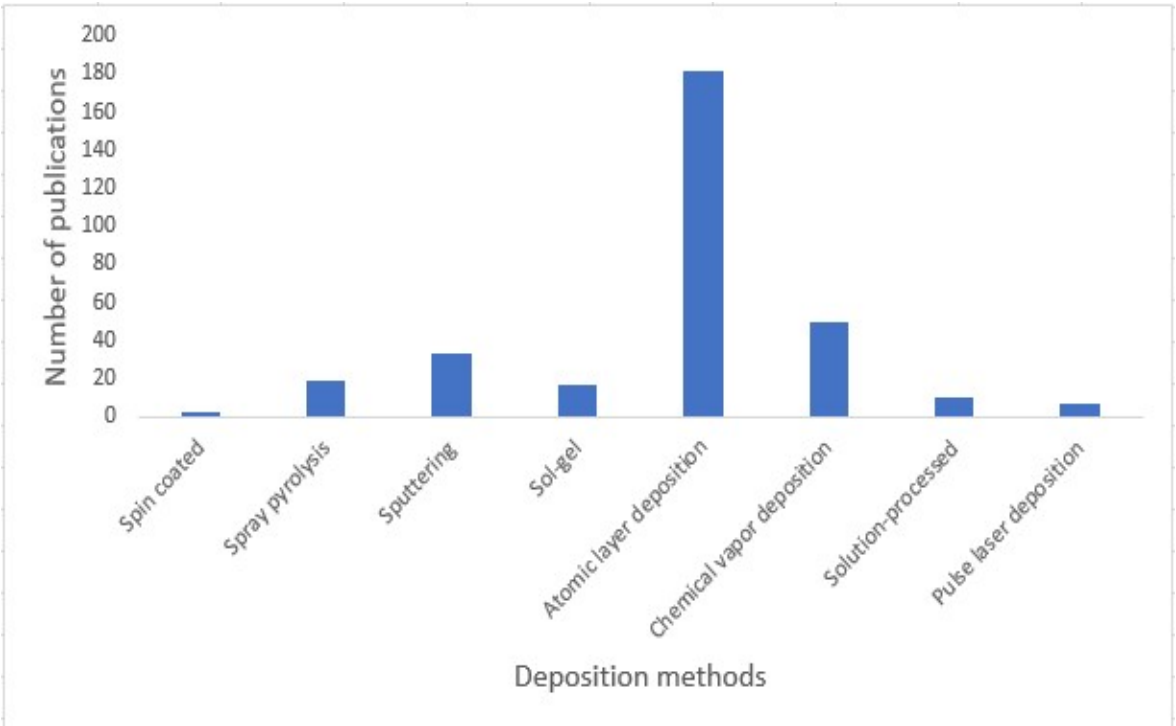

Figure 2.3 Schematic illustration of published methods used for deposition of AlO_x thin film in accordance to ISI web of knowledge database

2.3.1 Chemical deposition methods

The chemical deposition methods are described below;

Chemical vapor deposition: The CVD process was first used commercially for the deposition of pyrolytic carbon and metals in the late 1800s. Epitaxial deposition of silicon from SiH_4/H_2 on several metal oxide substrate surfaces was one of the earliest CVD studies to be documented in the Journal of Vacuum Science and Technology (JVST). In this deposition technique, solid thin films are deposited from the vapor phase through a chemical reaction. Wide range of nanomaterials like amorphous semiconductors, insulators, barrier layers, metals, silicides, superconductors, and organics can be deposited by this method [51].

The films deposited can either be epitaxial, polycrystalline or amorphous in nature. The films are employed in the fabrication of microelectronics and optoelectronic devices, they are also useful for optical coatings, protective coatings, and decorative coatings. This method is widely used due to the following advantages; they can be used to deposit new materials, thin films can be deposited over a wide range of deposition rates, it has the ability to exploit a variety of pressure conditions, films can be uniformly deposited over a large sample area, thin film properties and deposition

parameters can be controlled using the CVD process. Deposition parameters to be controlled are; process and film purity, doping level, stoichiometry, uniformity, layer thickness, interface abruptness, interface structure, conformality, film structure and crystallinity, and deposition selectivity [51]. For effective utilization of precursor in the CVD process, the precursor should: have adequate vapor pressure to allow transportation for film growth on the surface, undergo facile decomposition of the preferred product at a suitable temperature, have no reaction or association in the gas phase. Specialized aspect of the CVD processes are: epitaxial growth which is termed vapor phase epitaxy (VPE), organometallic vapor phase epitaxy (OMVPE)-for precursor containing a metal-carbon bond, deposition from a precursor that contains organic ligands attached to the metal such as alkoxides, amides, or diketonates are termed metalorganic chemical vapor deposition (MOCVD) process.

CVD equipment selection is strongly dependent on; the quality and type of film desired, the properties of the film that is of interest, chemistry selected for deposition, and the conditions needed to carry out the reaction process. CVD reactors can be classified by: (1) the number of wafers processed concurrently (batch or single wafer), (2) the arrangement of the wafer (stacked or planar), (3) the operating pressure of the reactor (UHV to atmospheric), (4) the wall temperature of the reactor (hot or cold wall), (5) the process of adding energy to cause deposition (thermal and/or plasma) [51].

Atomic layer deposition (ALD): It is a surface-controlled layer-by-layer deposition process involving alternating, self-limiting surface reactions to achieve controlled atomic level deposition. In order to have a successful ALD deposition, it is essential to devise a reaction scheme involving a sequence of discrete, self-limiting adsorption and reaction steps. Precursors for ALD should be highly reactive and contain surface termination groups that give rise to volatile by-products, but should additionally result in a self-limiting surface reaction mechanism [51]. The step involved in the ALD process are; reaction of the precursor containing metal or non-metal source atom, reduction, oxidation, or nitridation in the subsequent steps. Growth temperature is very important during the reaction and in the desorption of ligands and by-product because the ALD is a surface adsorption and reaction controlled process [51].

2.4 Chemical spray pyrolysis (CSP)

Spray pyrolysis technique is a very simple, non-vacuum and cost-effective method of preparing thin and thick films, ceramic coatings and powders [17], [68]. Thin film is deposited by spraying a precursor solution on a heated substrate, where the constituents vaporizes, and the precursor salt decomposes [69], [70].

It can be used to prepare films of any composition, high quality substrates or chemicals are not needed, substrates with multifarious shapes can be coated, it can also be used to produce uniform and high quality coatings [71]. Dense films, multilayered films, and porous films for powder production, have employed the spray pyrolysis technique for deposition. It has been widely employed for decades in the solar cell production and glass industry [17]. Chamberlin and Skarman were the first set of researchers to employ the spray pyrolysis technique in 1966 to deposit CdS films for solar cells. Since then, detailed research and investigation have been done on this method of deposition [70].

The spray pyrolysis technique setup consists of Atomizer, precursor solution, substrate heater, and temperature controller. There are 3 kinds of atomizers employed for the spray pyrolysis method viz; (i) Air blast (the solution is exposed to a stream of air) (ii) Ultrasonic (ultrasonic frequencies produce the short wavelength necessary for fine atomization) (iii) Electrostatic (the liquid is exposed to a high electric field) [17]. Atomizers vary according to its droplet size, rate of atomization and droplet velocity. Droplet velocity is significant because it can determine the heating rate and residence time of the droplet during spray pyrolysis. The size of the droplets produced with pneumatic or pressure nozzles decreases when the pressure difference across the nozzle is increased. Ultrasonic atomizers can produce droplets as low as 2 to 4 µm, but atomization rate can't exceed 2 cm^3/min [72]. For a specific atomizer, the droplet qualities depend on the solution density, viscosity, and surface tension. The viscosity of metal organic and organic acid precursors can vary in orders of magnitude, depending on chemistry.

Spray pyrolysis technique involves 3 major steps: Precursor solution atomization, Aerosol transportation, and decomposition of the precursor on the substrate. Having a good understanding of these processes helps to improve film quality [17]. Generally, in an experimental setup, the synthesis parameters that are more important are the concentration molarity of the precursor solution, the carrier gas flux rate, and the synthesis temperature [68]. Examples of aerosol precursors used are; True solutions, colloidal dispersions, emulsions and sols. However, aqueous solutions are regularly used due to ease of handling, safety, low cost, and its availability over a wide range of water-soluble metal salts [72].

Deposition parameters such as substrate temperature and spray rate affect the structure and properties of deposited films in spray pyrolysis method. Substrate surface temperature is the main parameter that influences film morphology and properties. Altering the temperature can change the film morphology from a cracked to a porous microstructure [17]. Solvent, type of salt, concentration of salt, and additives influence the physical and chemical properties of the precursor solution. Changing the composition of precursor solution and spray rate affects the structure and properties of a deposited film [17].

2.4.1 Ultrasonic spray pyrolysis method

The ultrasonic spray pyrolysis method was adopted in this thesis to deposit AlO_x thin film. In the ultrasonic spray pyrolysis system, an ultrasonic nebulizer is used to obtain evenly distributed micrometer and sub-micrometer size droplets. The nebulizer vaporizes the precursor solutions leading to formation of mist while being operated at a frequency of 2.56 MHz. The vapor is transported to the heated substrate via a carrier gas through a pipe. For large area substrate coating, small sized droplets with narrow size distribution are formed from the precursor solution through ultrasonic waves, the solvents vaporizes as the droplets hit the substrate, leading to the formation of thin solid films [18]. The schematic diagram explaining the ultrasonic spray pyrolysis technique is in Fig. 2.4 below.

2.4.2 Advantages and disadvantages of ultrasonic spray pyrolysis method

The ultrasonic spray pyrolysis technique offers both advantages and disadvantages in thin film deposition. The advantages of ultrasonic spray pyrolysis methods are; [18][73]

1. The gas flow rate doesn't depend on the aerosol flow rate unlike in the pneumatic spray system.

2. Small and homogenous droplet size distribution

3. Droplet size can be decreased by increasing ultrasonic frequency.

Disadvantages; [73][74]

1. Low throughput from the ultrasonic atomization

2. Spray nozzle may become cluttered after long deposition time.

3. It may lead to oxidation of sulphides when processed in air atmosphere.

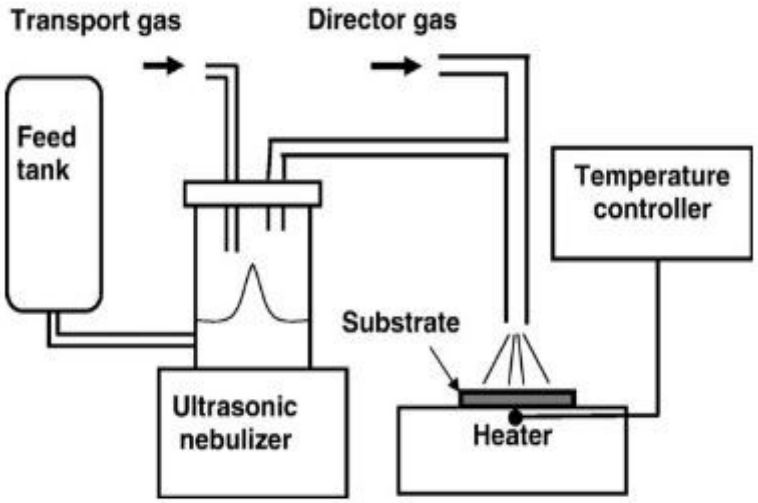

Figure 2.4 Schematic diagram of ultrasonic spray pyrolysis technique [75]

2.4.3 Applications of spray pyrolysis

Spray pyrolysis presents several opportunities to synthesize powders with modified physical and chemical characteristics. This technique can be used to synthesize solid particles to give well-defined properties required for the fabrication of advanced ceramics such as chemical purity and homogeneity, <1 µm particle diameter, dense particles, equiaxed shape, and freedom from particle aggregation. The main setback to using this technique for solid particles synthesis is the formation of hollow particles or broken shells [72].

Spray pyrolysis technique also offers the opportunity to synthesize hollow or porous particles that maybe valuable for thermal insulation or applications for catalyst support. Powders formed from metal nitrates consist of porous or irregular particles because molten salt inhibit removal of the entrapped solvent, since a number of metal nitrate melt before the solvent is completely removed [72]. Based on inherent simplicity and compositional flexibility, spray pyrolysis techniques have the possibility to expand the availability and compositional range of nanostructured particles.

A discontinuous fiber can be formed by spray pyrolysis when using a two-fluid atomizer by altering the precursor viscosity, surface tension and solution concentration. Spray pyrolysis is applicable for producing thin films of the desired stoichiometry on large and nonplanar surfaces. This technique has been widely applied to produce coating films of transparent conducting oxide, sulfide, and selenide semiconductors [72]. The spray pyrolysis technique has been used to deposit various thin films of materials such as Sb_2S_3 [76], TiO_2 [77], Sn_xS_y [78], and ZrO_2 [79], for several applications.

I. Dundar et al. [77] have presented the effect of change in deposition temperature on TiO_2 thin film, deposited by ultrasonic CSP on window glass substrate. They reported an increase in film thickness with increasing deposition temperature. The films deposited at the highest deposition temperature (450 ^oC) show visible large grains of approximately 50 nm, RMS roughness value of 1.2 nm with a total transmittance of 80% in the spectral region (400-800 nm), while the films deposited at lower deposition temperature were relatively smooth with little or no grains present, and a lower optical transmittance. A. Oluwabi et al. [79] also reported similar effect of deposition temperature on film thickness for ZrO_2 films as-deposited on quartz substrate.

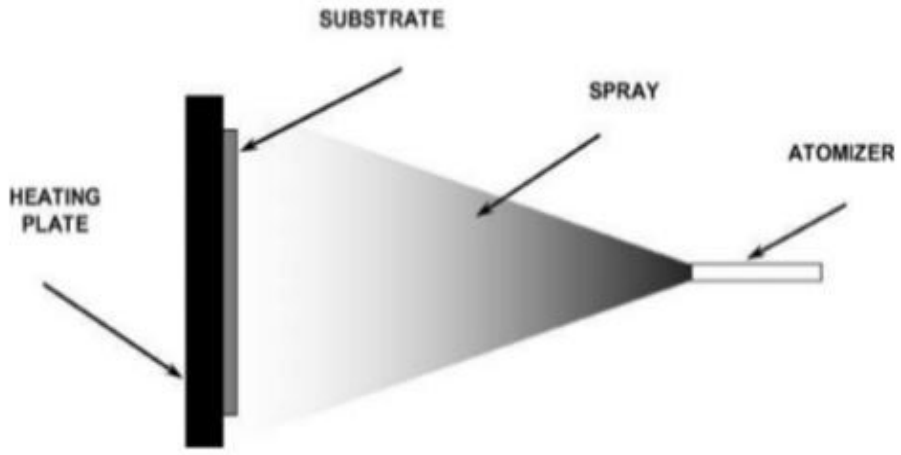

Figure 2.5 Schematic diagram of chemical spray pyrolysis setup [17]

2.5 Influence of deposition parameters on AlO_x thin films

Properties of thin films are greatly influenced by deposition parameters such as deposition temperature, precursor concentration and deposition rate.

It was reported by Kiyoto et. al [12] that absorption coefficient of chemical vapor deposited AlO_x film increases with increasing deposition temperature across the frequency ranges. Effect of heat treatment on absorption coefficient also depends on depends on deposition temperature.

According to the study by Yiquan et al., Alumina coatings deposited by aerosol assisted spray deposition with same deposition temperature (450 ^oC) but different molecular weight precursors were reported to have different color and microstructure. Alumina films with high molecular weight precursor of aluminum acetylacetonate were darker than alumina films with low molecular weight precursor of aluminum acetate. The dark color was due to the presence of carbon as a result of incomplete oxidation reaction of carbon [44].

Aguilar-Frutis et al. [10] have investigated the effect of spraying solution with and without the addition of water mist on AlO_x thin films deposited on silicon and quartz substrates by ultrasonic CSP technique. They reported that the films deposited with the addition of water mist produced the best films, with a low content of -OH and water related bond, and highest refractive index. Truong et. al also investigated the effects of substituting TMA precursor which is most common precursor material for atomic layer deposition with ATIP in deposition of AlO_x film. They observed that AlO_x film prepared by thermal ALD technique using ATIP and water precursor has a maximal growth per cycle of 1.8 Å/cycle at 150 ^oC temperature [47].

2.6 Influence of annealing process on AlO_x thin films

Annealing plays a significant role for the structural, electrical and optical properties of Aluminum oxide thin films.

Zhao et al. reported that aluminum oxide film deposited by filtered cathodic vacuum arc method and annealed at 900 ^oC showed monoclinic crystallinity induced by crystallization at such high annealing temperature [14]. It is unusual to have any degree of crystallinity in alumina thin films deposited or annealed at temperatures below 700 ^oC [43].

Yiquan et al. studied the microstructure of Alumina coating prepared by spray deposition method. They observed that the color of Alumina coatings heat-treated in air, at a temperature of 550 ^{o}C for 2 h changed from brown/grey to white [44]. Recently, Tang et al. [45] have also investigated the effects of annealing rate on sputtered AlO_x films. They reported that annealing rates can significantly change the phase of the AlO_x films from amorphous to crystalline. As-deposited AlO_x films annealed at 500 ^{o}C and further heat treated at 800 ^{o}C and 900 ^{o}C at a very high annealing rate resulted in crystallized film. However, at low annealing rate, the films were amorphous. Increasing annealing rate also led to a finer, more compact, and improved film surface for the film annealed at 500 ^{o}C. This result is also similar for films heated at 900 ^{o}C at a high annealing heat rate as they show an unbroken surface morphology.

WenWen et al. in their recent study also reported that increasing annealing temperature of AlO_x film deposited by the sol-gel method decreases the leakage current density of the film and vice versa. The reduced leakage current was attributed to the decrease in oxygen defect as Al-O bonding forms, and the large leakage current was due to the presence of hydroxyl group and residual organics which form the conduction paths. They also recorded a large dielectric value of 13.8 for low temperature annealed AlO_x film, which was ascribed to the large amount of hydroxyl group revealed by the XPS result [46].

2.7 Properties of AlO_x thin films by chemical deposition method

Several techniques have been reported for the chemical deposition of Aluminum oxide thin films such as; sol-gel, spin and dip-coating, atomic layer epitaxy, spray pyrolysis, chemical vapor deposition [17], and they are summarized in Fig. 2.4.

Yiquan et al. prepared AlO_x thin film on glass substrate by aerosol assisted spray deposition method at a deposition temperature of 450 ^{o}C. They reported that the film prepared using high molecular-weight precursor such as aluminum acetylacetonate was darker and less dense than that with low molecular weight aluminum acetate precursor. Annealing the films at 550 ^{o}C in air for 2 hours changed the film color from brown/grey to white [44].

Aguilar Frutis et al. reported that the addition of water mist during the spray deposition process led to an improvement in the overall dielectric properties of AlO_x films prepared from a solution of

aluminum acetylacetonate and N,N-dimethylformamide and deposited on silicon substrate at temperatures between 450 - 650 ^{o}C [10]. Wonjin et al. have demonstrated that AlO_x films deposited by plasma-enhanced chemical vapor deposition method at deposition temperature of 100 ^{o}C and 400 ^{o}C on silicon substrate before and after etching have a smooth surface [52].

Toshiro Maruyama et al. prepared amorphous AlO_x film by chemical vapor deposition on glass and silicon substrate which was heated to a temperature of 250 ^{o}C. They reported that the X-ray diffraction pattern of the films showed that the films were amorphous [11]. Wangying et al. reported that increase in annealing temperature decreases both the dielectric constant and leakage current of the sol-gel deposited AlO_x films. The film thickness increases with a decrease in annealing temperature. And the films were all amorphous until annealing temperature reaches 500 ^{o}C [6].

J-Guzman et al. studied the structural characteristics of AlO_x film deposited by spray pyrolysis with and without the addition of water mist on silicon substrate at a temperature in the range of 500 – 650 ^{o}C. They reported that AlO_x film without the addition of water mist are amorphous and porous nature, while the film with the addition of water mist results in a crystalline and denser material [9]

Ahmet et al. described the relationship between annealing temperature of films deposited by plasma-enhanced atomic layer deposition method and dielectric constant. Increasing the annealing temperature increases the dielectric constant of the annealed films from 8.5 to 10.2. The films were amorphous in the annealing temperature range of 250 – 750 ^{o}C with a dielectric constant of 8.5. At annealing temperature between 750 – 1000 ^{o}C, the films show a crystalline phase and this increased the dielectric constant to 10.2 [13].

With respect to the effect of atmosphere in which dielectric measurement is carried out, N. Koslowski et al. [53] revealed that dielectric measurements done in ambient temperature increases the capacitance significantly and affect parasitic resistance due to water molecules from the atmosphere adsorbed on the film surface. It was established that AlO_x films deposited by spin coating method at high humid conditions improves the electrical properties of the film by producing a smooth film surface, very low leakage current and higher breakdown voltage. At low humid conditions, spherulite structure in form of cracks are formed on the surface of the films leading to unfavorable dielectric properties [54].

It was reported by J. Jun et al. [55] that hydration improves the properties of AlO_x films. They discovered that increase in dipping time of AlO_x films in deionized water increases the dielectric constant from 7.8 to 11.5 with no significant increase in leakage current. This effect is due to the structural change of the film surface from aluminum oxide to pseudo-boehmite after reaction with

water. Kolodzey et al. [34] also confirmed the effect of difference in oxidation conditions, sublayer composition and structure in the variation of current-density characteristics. The summary of the properties of AlO_x thin film deposited by different chemical deposition methods as reported in literatures are listed in Table 2.5.

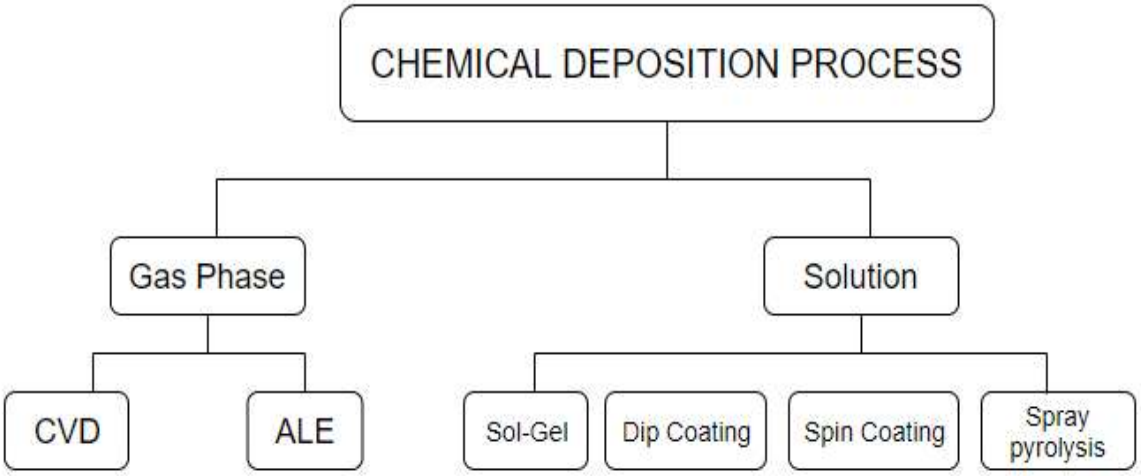

Figure 2.6 Chemical deposition methods [17]

Table 2.5 Summary of AlO_x films deposited by chemical methods

Deposition Method	**Precursor**	**Solvent**	**Substrate**	**Ts (°C)**	**Tan (°C)**	**Crystal structure**	**Dielectric constant**	**Resistivity (Ωcm)**	**Refractive Index**	**Ref.**
Spray pyrolysis	Aluminium acetylacetonate	N,N-dimethyl formamide	Silicon & Quartz	450-650		Amorphous				[10]
Sol-gel	Aluminium sec-butoxide	Anhydrous ethanol, isopropanol, and n-butyl alcohol	Borosilicate glass, Silicon	25	200, 500	Amorphous			1.54 - 1.60	[7]
Sol-gel	Aluminum nitrate nonahydrate	Ethanol	Silicon		100-500	Amorphous	8.7-157 @100 Hz			[6]
Sol-gel	Aluminium sec-butoxide	Isopropanol, acetyl-acetone	Quartz	25	500					[8]

Deposition Method	Precursor	Solvent	Substrate	Ts (°C)	Tan (°C)	Crystal structure	Dielectric constant	Resistivity (Ωcm)	Refractive Index	Ref.
Chemical vapor deposition			Silicon	400-1000	500-1300					[12]
Spray pyrolysis	Aluminum acetylacetonate	N,N-Dimethyl formamide	Silicon	500-650		with water mist: crystalline w/o water mist: amorphous			1.66	[9]
Chemical Vapor Deposition	Aluminum acetylacetonate		Borosilicate glass & Silicon, quartz	250-600					1.56	[11]
PEALD		TMA + Di oxygen precursor	Silicon	300	500 - 1100	Amorphous & crystalline	Am: 8.5 Polyc: 10.2			[13]
PECVD	Dimethyl aluminum isopropoxide		Silicon wafer	30 - 500						[52]
Spray pyrolysis	Aluminum acetylacetonate	Dimethyl formamide	Silicon, Steel, Nickel	300, 350		Amorphous		Steel: $5x10^{11}$	MOS @350: 9.6	[39]
Atomic Layer Deposition	TMA	Water	Graphene	200						[56]
Atomic Layer Deposition	TMA	Water	Silicon	200	350		10.5			[57]
Spin-coating	Aluminum nitrate hydrate	Deionized water			250					[54]
Atomic layer deposition	TMA		Silicon	RT, 100, 150			8.6-7.4			[58]

2.8 Applications of AlO_x thin films

AlO_x thin films are useful as dielectric layers in several types of microelectronic devices [10], as an anti-reflection coating and passivation film for silicon-based solar cells [40], biomedicine, neurosurgery, and optoelectronics [32].

They are suitable for optoelectronic and microelectronic devices due to their high mechanical strength, wear resistance, chemical inertness, good adhesion to glass substrate, transparency over wide wavelength [59], and their resistance to corrosive environments [32].

2.8.1 Solar cells

Schmidt et al. have studied the application of AlO_x thin films deposited by atomic layer deposition in solar cells. They reported that AlO_x thin film can function as antireflective coating and passivating layer in solar cells as it provides an excellent level of surface passivation on p- and n-type silicon wafers. It is the ideal choice for a dielectric layer at the c-Si solar cell rear because of its very high transparency for near-bandgap photons [60].

Ismail et al. reported that Silicon photodiode coated with nanostructured Alumina film gives a low optical reflectance. The least reflectance of the silicon photodiode was recorded for Alumina film prepared at 3.5 J/cm^2/pulse. The average optical reflectance of silicon decreased from 31 to 15% after alumina deposition, which is an indication of the effect of the antireflection properties of Alumina film. After deposition of Alumina films, the dark current of the photodiode decreases while the photodiode current increases [33].

Dobrzanski et al. have also studied the influence of AlO_x film as an antireflection coating on the efficiency of solar cells. They reported that AlO_x coating deposited on solar cell by atomic layer deposition method increases the fill factor, short circuit current, open circuit voltage, and efficiency of solar cells with efficiency difference of about 5.28% between solar cells with and without antireflective coating. Reflection accounts for about 8% loss in solar cells, therefore, reduced reflection leads to a much more improved efficiency of solar cells. Efficiency difference of 5.28% was reported for solar cells with and without antireflective coating [61].

2.8.2 Thin film transistors

In thin film transistors, Arunima et al. have shown that AlO_x can be used as a suitable substrate and dielectric layer for n-layer MoS_2 transistors. They reported that the use of AlO_x material for high gate dielectric can improve the stability and increase mobility in MoS_2 layers transistor [62].

Barbara et al. demonstrated that Aluminum oxide thin films modified with self-assembled monolayer can be effective as gate dielectrics to achieve low operational voltage in solution-processed organic field effect transistors. The need to device a means of fabricating solution based transistors with low operational voltage stems from the fact that most organic transistors function at voltages that are too high for use in aqueous environment [38]. Shao et al. studied the electrical characteristics of atomic layer deposition of hydrogen rich AlO_x at different temperatures as a dielectric material in IGZO-TFT. They concluded that the hydrogen rich AlO_x film as-deposited at room temperature is most suitable due to its high field-effect mobility, small subthreshold swing, low threshold voltage, a large on/off current ratio, and enhanced negative and positive gate bias stabilities. The hydrogen rich AlO_x film also led to effective passivation of interfacial states of a-IGZO/Al_2O_3 ascribed to hydrogen impurities released as a result of electrons generated during sputtering of IGZO [58].

2.8.3 Dynamic random access memory (DRAM)

According to Sivaramakrishnan et al., AlO_x is one of the most appropriate material for blocking dielectrics in high performance memory, embedded flash and DRAM applications. Blocking dielectric blocks the leakage of the stored charge from the floating gate of a flash memory. Use of AlO_x (hence, larger physical thickness) as blocking dielectric can minimize the charge leakage efficiently and withstand higher operating voltages, thereby enhancing the programming and erasing speeds of the flash memory. High-k dielectrics are the next best alternative to be used as IPD since the conventional material used SiO_2 has reached its physical limit [63].

2.8.4 Humidity sensor

Shamala et al. [39] studied AlO_x thin films prepared by spray pyrolysis for application in humidity sensor. They fabricated a Metal Oxide Semiconductor capacitor sensor to study the variation of capacitance as a function of relative humidity and temperature. Parameters like volume resistivity and breakdown electric field present the properties of a good dielectric film.

2.8.5 Corrosion protection

Potts et al. [42] have investigated the properties of ultra-thin film AlO_x deposited by plasma enhanced atomic layer deposition (PEALD) in comparison with AlO_x film deposited by thermal atomic layer deposition (TALD) on steel and aluminum for corrosion protection. They reported that AlO_x thin films deposited by PEALD gave a longer corrosion protection and the lowest porosity than TALD AlO_x film. So therefore, it is a promising technique to deposit thin films for corrosion protection and sealing.

2.9 Thin film transistor (TFT) structure and operation

A transistor is a device that is used to amplify or switch electronic signals. It is divided into bipolar and unipolar (field-effect transistor, FET) [64]. Basically, a thin film transistor comprises of three elements [65];

- Semiconductor or channel layer
- an insulating layer
- the electrodes [66]. They are three namely; source, drain and gate [64].

Although, organic semiconductors have been known since 1940s, but the first transistor based on an organic semiconductor was only reported in 1986 with a device made on an electrochemically grown polythiophene film. The possibility of fabricating organic TFT with small conjugated molecules was reported in 1989 with sexithiophene [66]. Interests in organic semiconductor and solution-processed inorganic semiconductors such as oxides for TFT have grown in recent times because such materials can be processed and deposited cheaply thereby lowering the cost of fabrication [64].

Semiconducting inorganic or organic conducting channel is devised between two ohmic contacts: the source and the drain [64]. The source and the drain are in contact with the semiconducting film at a small distance from each other [66]. The gate regulates the charge induced into the channel from the source to drain when the gate voltage is higher than a threshold voltage [64].

The gate material of a thin film transistor can be doped silicon, indium tin oxide (ITO), or other conducting materials. A dielectric material functions as the gate insulator or capacitor, and the channel is composed of semiconductor materials such as conducting polymers or metal oxides [64].

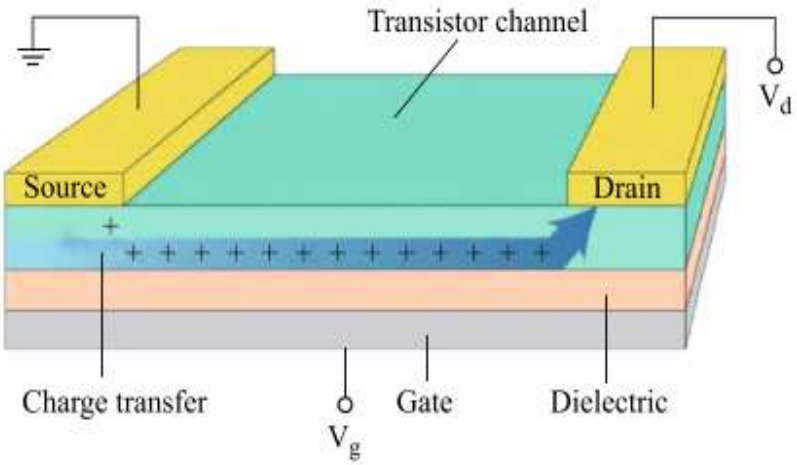

Figure 2.7 Schematic diagram of a TFT [64]

A thin film transistor functions as a capacitor, when a voltage is applied between the source and the drain, as shown in Fig. 2.7 above, a charge is induced at the insulator-semiconductor interface. The charge forms a channel which is conductive, and the conductance is proportional to the gate voltage. According to Ohm's law, at low drain voltage, current increases linearly with drain voltage. Insulator plays a vital role in the performance of a transistor by isolating the gate contact from the rest of the structure [66].

The TFT device is divided into two main groups; the staggered and coplanar group. This division is based on the configuration of the source/drain electrode and gate electrode. In the coplanar structure, the source/drain and gate electrodes are placed on the same side of the channel, and in the staggered structure, the source/drain and gate electrodes are placed at opposite sides. The TFT structure can be further classified into top-gate devices and bottom-gate devices depending on the position of the gate electrode [65], [67]. The bottom-gate devices are referred to as inverted structure [65].

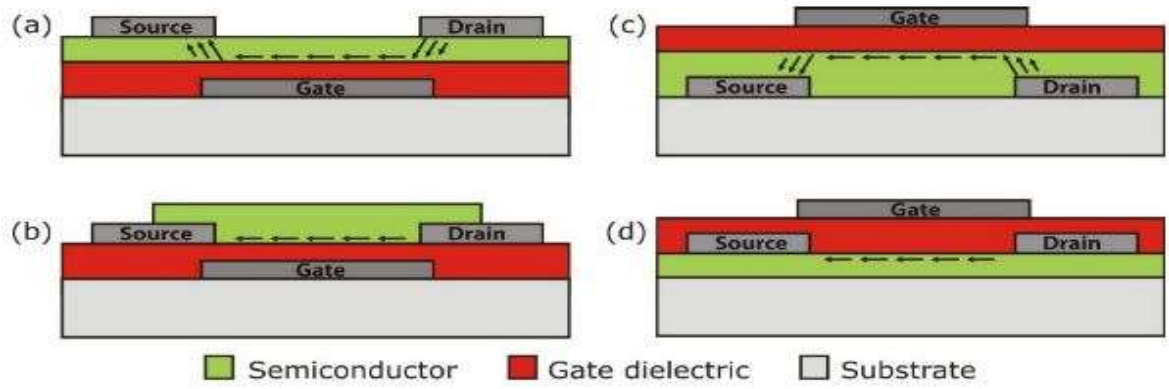

Figure 2.8 Thin-film transistor device (TFT) structures: (a) bottom gate, top contact, (b) bottom gate, bottom contact, (c) top gate, bottom contact, and (d) top gate, top contact [44]

Each of these TFT structures in Figure 2.8 has its advantages and disadvantages, and the type of structure adopted is a direct effect of its use. Bottom gate bottom contact structure offers the advantage of swift inspection and investigation of new semiconductor materials since the gate electrode, gate dielectric, source and drain contacts are pre-fabricated, and the semiconductor is deposited in the last stage of the process. A perfect semiconductor-dielectric interface can also be maintained as there are no other steps involved after depositing the semiconductor. The disadvantage of this structure is that it exposes the semiconductor to ambient conditions which may hasten degradation due to oxygen, water, and other factors. The Top gate top contact and top gate bottom contact structures make use of the dielectric material as an encapsulation layer to protect the semiconductor from environmental degradation. However, the dielectric material must be carefully chosen to preserve the integrity of the semiconductor [67].

Structure of organic semiconductors differs from that of inorganic semiconductors. Organic solids are defined by weak van der Waals bonds, in contrast to semiconductors like Silicon or Germanium, where covalent bonds define their crystals. This major difference has an impact on their properties and processing. Inorganic compounds are processed in extreme conditions such as high temperature and vacuum, while organic compounds are processed at or around room temperature and ambient pressure by inkjet processing, laser printing, or other simple methods due to the weak bonding present in organic materials [67].

The downside to the usage of SiO_2 as a dielectric material in TFTs is that the chemical structure contains a huge amount of surface states which can act as charge traps, thereby affecting efficient application of the device. Passivation of the Silicon oxide surface is one way to evade the effects of the traps. Charge scattering and density of traps can be limited in the electronic channel by minimizing the roughness at the semiconductor-dielectric interface. TFT operation is dependent on

the application of 2 potentials, which are the gate electrode and the drain electrode resulting into gate-source voltage (V_{GS}) and the drain-source voltage (V_{DS}) [67].

2.10 Summary of literature review and aim of the study

According to the literature review, Aluminum oxide has shown to be a promising material for use in the microelectronics industry due to its excellent insulative properties, high band gap, high dielectric material, wide transparency window from ultraviolet to mid-infrared region, good thermal and chemical stability, and superior electrical and mechanical properties. Aluminum oxide has been used in various applications such as for water purification, firebricks, integrated circuit, abrasives, anti-reflection coating, sensors, gas diffusion barrier, biomedicine and neurosurgery.

AlO_x thin films have also been deposited using various deposition methods such as spray pyrolysis, sol-gel, pulsed laser deposition, chemical vapor deposition, filtered cathodic vacuum arc, plasma-enhanced chemical vapor deposition, vacuum evaporation, and plasma-enhanced chemical vapor deposition. The most frequently used precursor material for deposition of AlO_x film is Aluminum acetylacetonate, and the most widely used deposition method is the atomic layer deposition method. However, there is limited publication on the dielectric applications of ultrasonic spray deposited Aluminum oxide films.

Ultrasonic spray pyrolysis (USP) deposition method is a very important technique for AlO_x thin film deposition because of its low-cost setup, simplicity and flexibility. It can be used to deposit homogenous thin films. Extensive study carried out on AlO_x thin films has shown it to be a versatile material. Aluminum oxide thin film has been used as an antireflective and passivating layer in solar cells to improve the efficiency of the cells. It is used as a suitable substrate and dielectric layer for gate insulator in Thin Film Transistors (TFT) to reduce leakage current and increase breakdown voltage for optimal performance of the TFT. Thin films of Aluminum oxide can also be used a blocking dielectric in performance memory, embedded flash and dynamic random access memory (DRAM) applications.

2.10.1 Aim of the study

The aim of the study is to fabricate Aluminum oxide thin films by ultrasonic spray pyrolysis technique for dielectric applications.

The objectives of the study are;

1. To deposit AlO_x thin films by chemical spray pyrolysis at various deposition temperatures.

2. To investigate surface morphology and structural characteristics of AlO_x thin films.

3. Analyse the electrical properties of the deposited AlO_x thin films.

3.0 MATERIALS AND METHODS

3.1 Experimental details

3.1.1 Reagents

The following reagents listed in Table 3.1. below were used in depositing thin films of Aluminum oxide.

Table 3.1 Details of chemicals used for the experiment

Reagent name	Chemical formulae	Molecular weight (g/mol)	Company	Purity (%)
Ethanol	CH_2H_5OH	46.07	Ou Estonian spirit	96.6
Methanol	CH_3OH	32.04	Sigma Aldrich	96
$Al(acac)_3$	$Al(C_5H_7O_2)_3$	324.31	Aldrich	99
Deionized water	H_2O	18.7	Milipore	>18.2 MΩ.cm

3.1.2 Preparation of precursor solution

In this experiment, the chemicals used for the preparation of the spray solution were methanol (solvent) and aluminium acetylacetonate (precursor). 50 ml volume of AlO_x solution with 0.05 M concentration was used for the deposition of films on all substrates irrespective of the deposition temperature. The solution was prepared by weighing a sample of 4.05 g of Aluminum acetylacetonate powder, this sample was dissolved in methanol to prepare a volume of 250 ml solution. The mixture was then stirred with a magnetic stirrer for 15 minutes at room temperature to ensure a complete dissolution and homogenous mixing. The steps involved in this preparation can be seen in the schematic diagram in Figure 3.1 below.

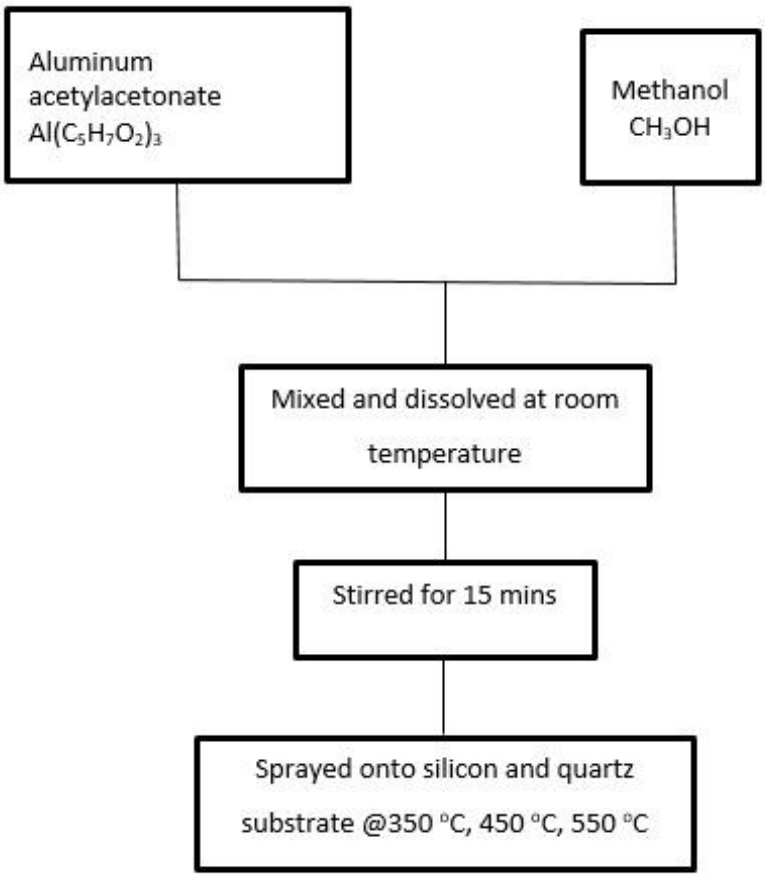

Figure 3.1 Schematic diagram for the preparation of spray solution

3.1.3 Substrate preparation

The substrates used for the purpose of this experiment were UV grade quartz (PGO-Germany) and an n-type silicon wafer of low resistivity (<0.005 ohm/cm from Siegert wafer). They were cut mechanically into sizes of dimension 2 cm x 1 cm. Afterwards, the substrates were cleaned for 5 minutes each at 60 °C with methanol, ethanol and deionized water in ultrasonic bath. Finally, the cleaned substrates were then dried in air and kept in a Petri-dish.

3.2 Deposition of AlO_x thin film

The cleaned substrates were placed on the heater and positioned in such a way that the vapor coming from the pipe will be evenly deposited on the substrates. The heater was allowed to heat

up to the required deposition temperatures (350 °C, 450 °C, and 550 °C) before depositing. The temperature of the heater is adjusted with the aid of the temperature controller. After reaching the desired temperature, it was left for few minutes to stabilize before plugging the ultrasonic generator.

The carrier gas flow rate used for spraying the solution was 3 L/min. The nebulizer was first calibrated using methanol as the spraying solution since the solvent used is methanol. The spray parameters were set at 3 steps, 10 cycles for deposition of 50 ml volume of AlO_x solution. Deposition parameters of AlO_x thin films on different substrates is shown in Table 3.2 below.

Table 3.2 Deposition parameters of the AlO_x thin films deposited by ultrasonic spray pyrolysis method

Sample name	**Substrate**	**Condition**	**Substrates Temperature (°C)**	**Carrier gas flow rate (L/min)**
1.1	Quartz	0.05 M	350	3
1.2	Quartz	Concentration	450	3
1.3	Quartz	of AlO_x	550	3
2.1	Silicon	10 cycles	350	3
2.2	Silicon	3 steps	450	3
2.3	Silicon		550	3

3.3 Annealing of AlO_x thin films

The AlO_x thin films deposited at 350 °C, 450 °C, and 550 °C on quartz substrates were annealed in air for 1 hour at temperatures of 500 °C, 800 °C, and 1000 °C using a Nabertherm L5/11/06D furnace. The films were first placed in the oven before setting the annealing temperature and annealing time. The heating time up to the required temperature was set for 20 minutes. After annealing, the films were allowed to cool down in the furnace before taking them out. Description of the annealing conditions is shown in Table 3.3 below.

Table 3.3 Annealing conditions of AlO_x thin films

Sample name	Substrate	Ts (°C)	Tan (°C)	Time (hour)
1.1a	Quartz	350	500	1
1.2a	Quartz	450	500	1
1.3a	Quartz	550	500	1
1.1b	Quartz	350	800	1
1.2b	Quartz	450	800	1
1.3b	Quartz	550	800	1
1.1c	Quartz	350	1000	1
1.2c	Quartz	450	1000	1
1.3c	Quartz	550	1000	1

3.4 Electrode deposition

Pure Aluminum metal electrode contacts were deposited on the surface of the as-deposited AlO_x film with silicon substrate with the aid of Quorum K975X vacuum evaporator to prepare the samples for electrical measurement. Before deposition was done, the surface of the film was covered with a mask of uniform area 1.7 mm^2. The samples were heated at 200 °C for 10 minutes. This experimental procedure was carried out in Laboratory of chemical thin film technology, Tallinn University of Technology, Estonia.

3.5 Thin film characterization methods

In this thesis, the characterization methods used were scanning electron microscopy (SEM), x-ray diffraction (XRD), current-voltage and impedance measurement.

3.5.1 X-ray diffraction

The structural properties and phase composition of the AlO_x thin films deposited on the quartz substrates was studied by carrying out x-ray diffraction measurement using an ULTIMA IV Rigaku D/max 2500 diffractometer and strip silicon detector D/Tex Ultra with Cu Kα radiation operated with 40 KV and 40 mA. The diffraction patterns were measured in the 2Θ range from 20 to 60 degree with a step of 0.02° and a scanning speed of 5 degrees/minute.

3.5.2 Current-voltage measurement

Electrical properties of AlO_x films were characterized by constructing a capacitor of AlO/AlOx/Si structure. The MOS structure was formed by evaporating Aluminum on the surface with 1.7 mm^2 as the contact area. The current-voltage (I-V) curves were measured by using the AUTOLAB PGSTAT30 in the Laboratory of Chemical Thin Film Technologies, Tallinn University of Technology. While the data was obtained by using the Frequency response analyser software. DC measurement was carried out by using graphite contact deposited on top of the AlO_x films. Resistance was determined from the inverse of slope of the I-V plot. Electrical resistivity was estimated from resistance using equation 3.1 below.

$$\rho = R \frac{A}{L} \qquad (3.1)$$

where ρ - resistivity, Ω cm,

L - film thickness, mm,

A - contact area, mm^2,

R – resistance, Ω.

The values for electrical conductivity was calculated by taking inverse of resistivity.

3.5.3 Impedance spectroscopy

The impedance measurement was done by using the AUTOLAB PGSTAT30 equipment. Capacitance was extracted from the impedance measurement and both the average area capacitance and average dielectric constants were estimated for all working devices at different frequencies. The Capacitance of the samples were estimated from the imaginary part of the impedance spectroscopy using equation 3.2 and dielectric constant in equation 3.3.

$$C = \frac{1}{2\pi f Z''} \quad (3.2)$$

where C – capacitance,

f - frequency, Hz,

Z” - imaginary impedance, Ω,

π - constant 3.1415.

$$C = \frac{\varepsilon_o k A}{d} \quad (3.3)$$

where C - capacitance,

ε_o - permittivity of free space,

k - dielectric constant,

A - contact area, mm^2,

d - film thickness, mm.

3.5.4 Scanning electron microscopy

The surface morphology and cross-sections were investigated with the aid of Zeiss HR FESEM Ultra 55 high-resolution scanning electron microscopy (SEM). The accelerated voltage for SEM measurement was 4.0 kV. SEM images were taken by focusing the samples on the electron beam where the electrons are made to relate with atoms in the sample. The apparatus consists

of the electron gun unit, scanning unit, demagnification unit, focus unit and detector unit. The measurements were carried out in the Laboratory of Optoelectronic Materials Physics by Dr. V. Mikli.

4.0 RESULTS AND DISCUSSIONS

4.1 Surface morphology

Figure 4.1 shows the surface morphology with cross-section of AlO_x films grown at 350 ^oC, 450 ^oC and 550 ^oC on quartz substrate. The images obtained from the SEM measurement were used to study the influence of varying deposition temperature on the as-deposited AlO_x film morphology and thickness. The surface of the films deposited were homogenous, well compacted and smooth. According to Alexey et al. AlO_x thin film deposited by atomic layer deposition method also show smooth surface [80].

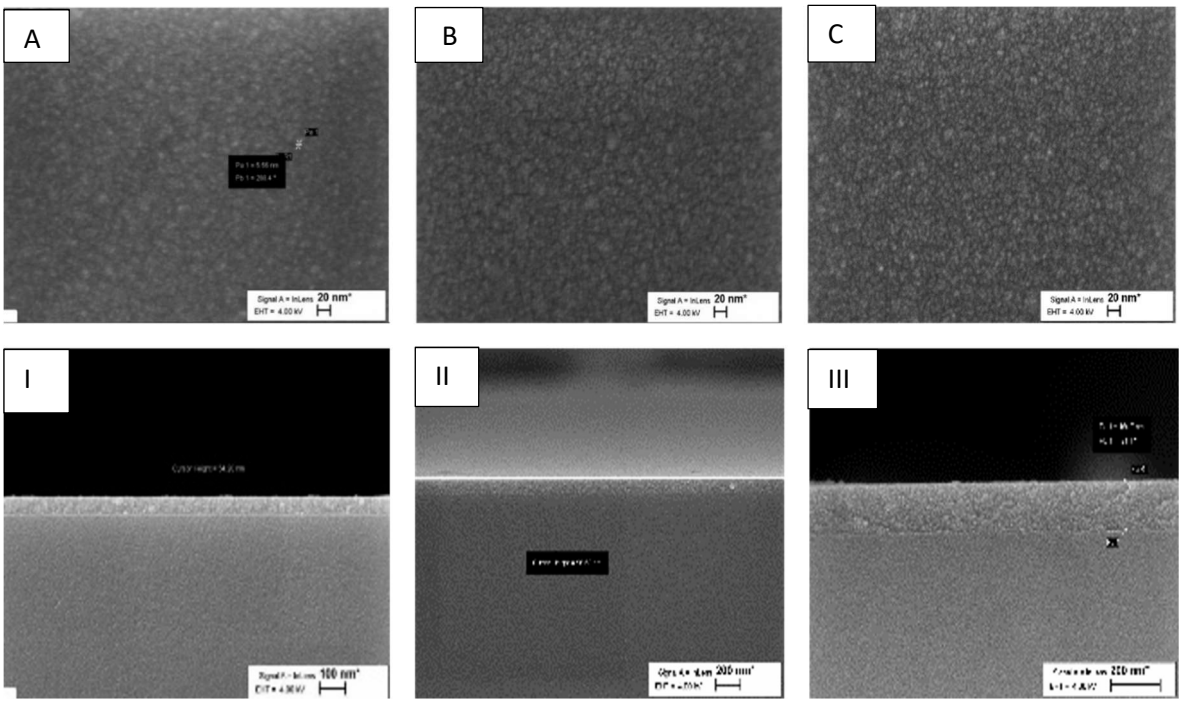

Figure 4.1 SEM images with cross-section of 0.05 M concentration of AlO_x as-deposited at 350 ^oC (A-I), 450 ^oC (B-II), 550 ^oC (C-III)

The thicknesses of the films were estimated from the cross-sectional images shown in Figure 4.1 (I-III). The obtained results revealed that the thicknesses of the films increase with increase in deposition temperature. The thickness of the film as-deposited at 350 ^oC is 54 nm, while the thickness of films as-deposited at 450 ^oC and 550 ^oC are 96 nm and 159 nm respectively.

4.2 Structural properties of AlO_x films

The X-ray diffractogram of AlO_x films as-deposited at 350 °C and 450 °C and annealed at 1000 °C on quartz substrates is shown in Figure 4.2. No diffraction peaks are observed in the XRD. This proves that all the samples were amorphous with no degree of crystallinity in the films. Amorphous films are desirable for application as a dielectric material where grain boundaries at crystalline interfaces can act as preferential paths for impurity diffusion and thus leakage currents, leading to a poor performance of the desired dielectric [53]. Our result corresponds with XRD measurements of AlO_x films in previous literatures that no sharp peak was observed for AlO_x film annealed until annealing temperature of 1000 °C [53][46][12].

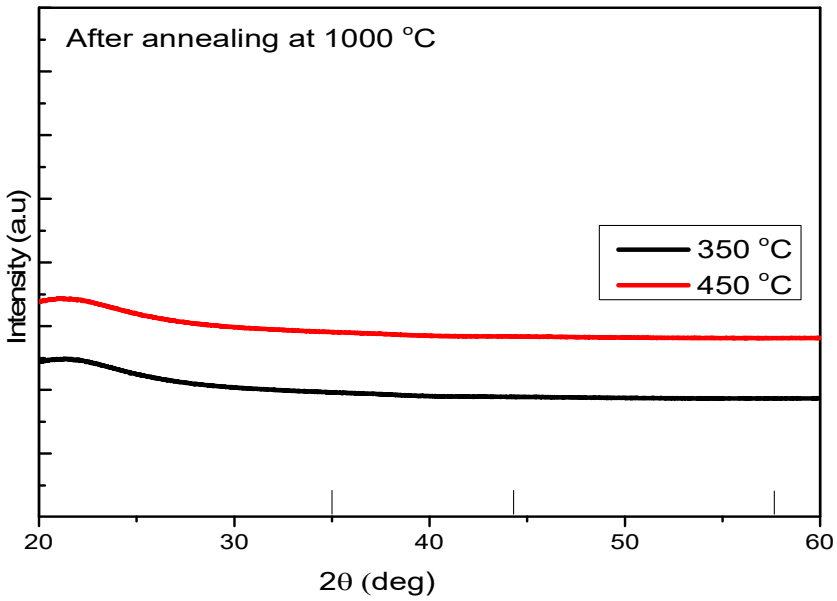

Figure 4.2 X-ray diffractogram of AlO_x thin films deposited at 350 °C and 450 °C, annealed at 1000 °C

4.3 Electrical properties

4.3.1 Current-voltage study of AlO_x thin films

Figure 4.3 shows the leakage current density in the forward bias and reverse bias regime (-2 V to +2 V). Electrical properties of the AlO_x films were characterized by constructing a capacitor of $Al/AlO_x/Si$ structure. The current density at -1.0 V was estimated to be 9.5×10^{-8} A/cm^2, 1.5×10^{-5} A/cm^2, and 1.6×10^{-6} A/cm^2 for AlO_x as-deposited at 350 °C, 450 °C, and 550°C respectively. J. Jun et

al. [55] reported a leakage current of 3.8×10^{-4} A/cm^2 for as-deposited AlO_x thin film by metal organic chemical vapor deposition. Y. Koda et al. [81] also reported leakage current density of 3.6×10^{-10} A/cm^2 for as-deposited AlO_x films. Our leakage current values are close to the values reported in previous literatures. The devices made from as-deposited AlO_x at both 450 °C and 550 °C have large leakage current densities attributed to the presence of large amount of residuals which will lead to conduction paths [6].

It can be seen from the result that AlO_x thin film as-deposited at 350 °C has a very small leakage current. This small leakage current could be attributed to a smooth and compact surface of the sample due to the absence of grain boundaries which may act as leakage channel resulting in a large leakage current. Presence of Al-O bonding on the film surface as a result of film condensation at higher deposition temperature also decreases the leakage current of dielectric layer [46]. It also shows that 350 °C deposition temperature could presumably be sufficient to achieve a good dielectric with low leakage current by using USP technique.

The resistivity values for the as-deposited AlO_x thin films were estimated to be 3.1×10^4 Ωcm, 1.6×10^5 Ωcm, and 3.9×10^1 Ωcm at 350 °C, 450 °C and 550 °C. It can be observed that AlO_x thin films as-deposited at 450 °C has a large electrical resistivity among all the samples which could be due to its small thickness. The resistivity of the film increases with increasing deposition temperature from 350 °C to 450 °C, followed by a decrease in resistivity with increase in deposition temperature from 450 °C to 550 °C.

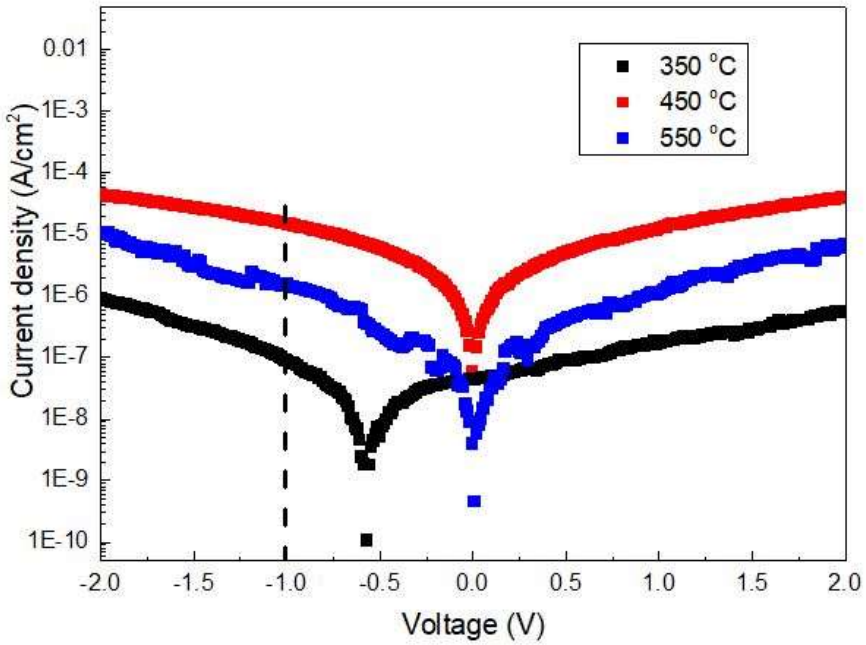

Figure 4.3 Leakage current density for AlO_x thin films as-deposited at 350 °C, 450 °C, and 550 °C

Performance of the TFT is strongly dependent on the breakdown properties and current transport behaviors of the gate dielectric films. The current transport in dielectric films is influenced by film material composition, film processing conditions, film thickness, trap energy level and trap density in the films [82]. Two transport mechanisms that are known to be important for tunneling in gate dielectric films are described below; Fowler-Nordheim tunneling and Frenkel-Poole emission [34].

- **Fowler-Nordheim (FN) tunneling:** They explain the phenomenon behind electrons tunneling from the metal into the conduction band of the dielectric material [34], [82]. Conduction current in dielectric films can be excellently described by the FN formula in the equations below.

$$J = CE^2 \, exp(-\beta/E) \qquad (4.1) \quad [82]$$

$$C = \frac{q^3 m}{16\pi^2 h m \emptyset} \qquad (4.2)$$

$$\beta = \frac{4}{3} \frac{(2m)^{1/2}}{qh} \emptyset^{3/2} \qquad (4.3)$$

where E – externally applied field,

q – electron charge,

m_e – electron mass in free space,

m_{ox} – electron mass in the oxide,

h – reduced planck's constant,

$\emptyset_o$ – barrier height, eV.

The conduction behavior in the conventional SiO_2 films has been extensively explained using the FN formula [82].

- **Internal Schottky (or Pool-Frenkel) effect:** It describes the field enhanced thermal excitation of electrons from its delocalized state into the conduction band of the insulator [34]. Dependence of current density on the oxide electric field is given by the equation below.

$$J = cE_{ox}exp[((dE_{ox})^{1/2} - \emptyset_t)q/K_bT] \quad (4.4)\ [34]$$

Where K_b – boltzmann's constant,

T – measurement temperature,

c – a constant that depends on the trap density,

d - $\frac{q}{\pi Ei}$,

E_i - total electric permittivity of the insulator.

Poole-Frenkel effect is clearly dependent on temperature. The higher the temperatures, the lower the current and the effect of the field on the current. Meanwhile, temperature dependence of the bandgap, the barrier heights, and the carrier occupation statistics have an effect on both current transport mechanisms [34].

4.3.2 Dielectric characterisation

Statistical studies of both the capacitance and dielectric values for about 30 capacitors were carried out after measuring the electrical impedance at a frequency range of 10 – 1 MHz. Capacitance value was extracted from the impedance and both the mean area capacitance and mean dielectric constants were estimated at different contacts for all working devices at different frequencies. The capacitance-frequency for as-deposited AlO_x thin films on silicon substrates presented on a box plot is shown in Figure 4.4. This plot shows the range of calculated area capacitance values for all the samples at different frequencies of 1 kHz, 10 kHz, and 100 kHz. It is seen that capacitance of AlO_x film as-deposited at 350 ^oC decreases with increase in the frequency. This phenomenon of reduced capacitance at high frequency is linked to the presence of trap states in dielectric films which prevents the film from acquiring enough speed needed to match higher frequencies [26]. On the other hand, capacitance values for AlO_x as-deposited at 450 ^oC and 550 ^oC were relatively stable across the frequency range. The variation in capacitance could be attributed to the presence of hydroxyl groups in the AlO_x films. Large amount of hydroxyl groups could lead to significant decrease in capacitance and vice versa [46].

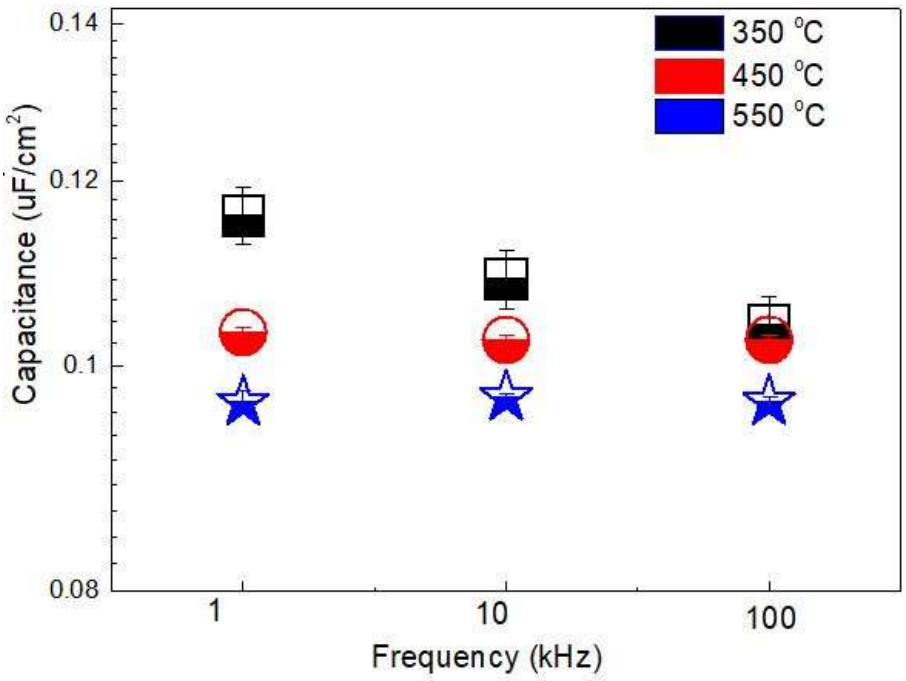

Figure 4.4 Capacitance-frequency plot for the AlO_x as-deposited on Si at 350°C, 450°C and 550 °C

AlO_x film as-deposited at 350 °C, 450 °C, and 550 °C at 1 kHz exhibited capacitance values of 116 nF/cm^2, 57 nF/cm^2, and 36 nF/cm^2 respectively. Area capacitance reported by Wenwen et al. [46] for annealed AlO_x films were in the range of 72.2 -120.6 nF/cm^2. It was also observed that the capacitance values decrease with increase in deposition temperature.

Figure 4.5 shows the dependence of dielectric constant on frequency for as-deposited AlO_x samples on silicon substrates. It was observed that the capacitor with as-deposited AlO_x thin film at 350 °C has a large dielectric constant value of approximately 7.4 at 1 kHz. Reported values of dielectric constant for as-deposited AlO_x films are in the range of 7-10 [83][19]. At higher frequency dispersion, mean dielectric constant for sample as-deposited at 350 °C is almost equal to that of the sample as-deposited at 550 °C. The summary of the electrical results are presented in Table 4.1 below.

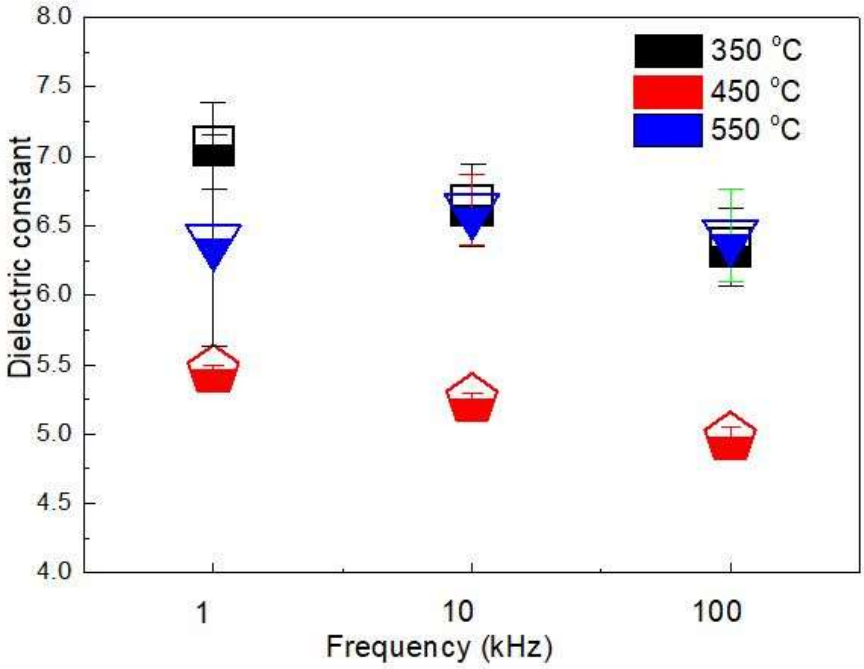

Figure 4.5 Dielectric-frequency plot for the AlO_x as-deposited on Si at 350 °C, 450 °C and 550 °C

Table 4.1 Summary of the electrical results for as-deposited AlO_x samples

As-deposited Samples (°C)	**Thickness (nm)**	**Area (cm^2)**	**Dielectric constant @ 1kHz**	**Capacitance (nF/cm^2) @1kHz**
350	54	0.017	7.4	116
450	96	0.017	5.6	57
550	159	0.017	6.5	36

4.4 Recommendations for future work

In this research work, it has been established that AlO_x thin film as-deposited at 350°C by ultrasonic spray deposition (USP) method has excellent properties that makes it desirable as a dielectric material. However, the electrical properties of annealed AlO_x films have not been studied. The following recommendations are useful for future research in this field:

(1) It is recommended that the performance of thermal annealed AlO_x films deposited by USP as a dielectric layer should be studied.

(2) XPS and EDX characterization should be carried out on the as-deposited AlO_x films to study the elemental composition and stoichiometry of the films.

(3) The as-deposited AlO_x thin films should be tested in a TFT.

5.0 SUMMARY

In this thesis, chemical spray pyrolysis deposition method which is cheap and allows mixing of precursor solution prior to deposition was adopted to deposit thin films of amorphous AlO_x at deposition temperatures of 350 ^oC, 450 ^oC, and 550 ^oC onto a preheated silicon and quartz substrates. The influence of varying deposition temperature and annealing temperature on the AlO_x film's structural, morphological and electrical properties for application as a dielectric layer in thin film transistor technology were investigated. The experiments were carried out in the Laboratory of Thin film Chemical Technology, Tallinn University of Technology. The results of this research have been presented at the 16th International Conference of Young Scientists on Energy Issues (24.05.2019 - 25.05.2019), in Lithuania and published in proceedings of ISSN 1822-7554. Conclusions drawn from this research is based on experimental observation supported and backed by results from other literatures reviewed on AlO_x films deposited by other deposition techniques.

The conclusions are summarized below:

- AlO_x thin films was successfully deposited by the CSP method at different deposition temperatures.
- The SEM study revealed that the AlO_x films as-deposited by the chemical spray pyrolysis technique were homogenous, compact and smooth. The film thicknesses increase with increase in deposition temperature. The thickness of the as-deposited films were in the range of 54 nm – 159 nm.
- XRD data revealed that both the as-deposited and annealed AlO_x films on quartz substrate were amorphous with no degree of crystallinity in the films.
- Resistivity of the as-deposited AlO_x films on Silicon substrate are in the range of 10^1 Ωcm - 10^5 Ωcm, and resistivity increases with increasing deposition temperature from 350 ^oC – 450 ^oC. Leakage current density at -1.0 V were in the range of 10^{-8} A/cm^2 – 10^{-5} A/cm^2. AlO_x thin film as-deposited at 350 ^oC has noticeably small leakage current which could be attributed to a smooth and compact surface of the sample due to the absence of grain boundaries which may act as leakage channel resulting in a large leakage current. Decrease in leakage current could also be due to the presence of Al-O bonding on the film surface as a result of film condensation at higher deposition temperature.
- Dielectric study revealed that at frequency of 1 kHz, the dielectric constants for the as-deposited AlO_x films were in the range of 5.6 – 7.4, and area capacitance values are in the range of 36 – 116 nF/cm^2. Both the area capacitance and dielectric constant decrease with increase in deposition temperature. Reduced capacitance at high frequency is linked to the

presence of trap states in dielectric films which prevents the film from acquiring enough speed needed to match higher frequencies. Variation in capacitance could also be due to the presence of hydroxyl groups on the film's surface.

- Finally, we can conclude that AlO_x films deposited at 350 ^oC by chemical spray pyrolysis method are desirable for superior performance as a dielectric layer in thin film transistors due to its smooth surface and amorphous nature, large resistivity, small leakage current, and a very large dielectric constant.

ACKNOWLEDGEMENTS

This study was financially supported by the Estonian Ministry of Education and Research, project IUT19-4, and by the European Union through the European Regional Development Fund, project TK141 ‘Advanced materials and high technology devices for energy recuperation systems’.

LIST OF REFERENCES

[1] H. Wang, T. Sun, W. Xu, “RSC Advances dielectric for combustion derived oxide thin film,” no. 3, pp. 54729–54739, 2014.

[2] A. F. Paterson and T. D. Anthopoulos, “Enabling thin-film transistor technologies and the device metrics that matter,” *Nat. Commun.*, vol. 9, no. 1, p. 5264, 2018.

[3] P. Nilai and N. Sembilan, “International Journal of Chemical Preparation of Nanocrystalline Aluminum Oxide Thin Films : A Review,” vol. 15, no. 2, pp. 1–8, 2018.

[4] J. Cui, M. G. Kast, B. A. Hammann, Y. Afriyie, K. N. Woods, P. N. Plassmeyer et. al, “Aluminum Oxide Thin Films from Aqueous Solutions: Insights from Solid-State NMR and Dielectric Response,” *Chem. Mater.*, vol. 30, no. 21, pp. 7456–7463, 2018.

[5] P. Katiyar, C. Jin, and R. J. Narayan, “Electrical properties of amorphous aluminum oxide thin films,” vol. 53, pp. 2617–2622, 2005.

[6] W. Xu, H. Wang, F. Xie, J. Chen, H. Cao, and J. Bin Xu, “Facile and Environmentally Friendly Solution-Processed Aluminum Oxide Dielectric for Low-Temperature, High-Performance Oxide Thin-Film Transistors,” *ACS Appl. Mater. Interfaces*, vol. 7, no. 10, pp. 5803–5810, 2015.

[7] N. Avci, P. F. Smet, J. Lauwaert, H. Vrielinck, and D. Poelman, “Optical and structural properties of aluminium oxide thin films prepared by a non-aqueous sol – gel technique,” pp. 327–333, 2011.

[8] A. Korcala, P. Płóciennik, A. Zawadzka, and B. Sahraoui, “Optical Properties of Al 2 O 3 Thin Film Deposited by Sol-Gel Technique,” pp. 3–4, 2015.

[9] J. Guzman-Mendoza et. al, “Structural characteristics of Al_2O_3 thin films prepared by spray pyrolysis,” no. 111, 2001.

[10] M. Aguilar-frutis, M. Garcia, C. Falcony, G. Plesch, and S. Jimenez-sandoval, “A study of the dielectric characteristics of aluminum oxide thin films deposited by spray pyrolysis from Al Ž acac . 3,” pp. 200–206, 2001.

[11] T. Maruyama and S. Arai, “Aluminum oxide thin films prepared by chemical vapor deposition from aluminum acetylacetonate Aluminum oxide thin films prepared from aluminum acetylacetonate by chemical vapor deposition,” vol. 322, no. 1992, pp. 1998–2000, 2013.

[12] Kiyoto Iida, “Physical and Chemical Properties of Aluminum Oxide Film Deposited by Iida_1972_Jpn._J._Appl._Phys._11_840.pdf.” Japanese Journal of Applied Physics, 1972.

[13] A. Lale, E. Scheid, F. Cristiano, L. Datas, and B. Reig, “Study of aluminium oxide thin fi lms deposited by plasma-enhanced atomic layer deposition from tri-methyl-aluminium and dioxygen precursors : Investigation of interfacial and structural properties,” vol. 666, no. December 2017, pp. 20–27, 2018.

[14] Z. W. Zhao, B. K. Tay, “Property Study of aluminium oxide thin films by thermal annealing,” pp. 550–551, 2010.

[15] S. Kalaivani and A. Kottantharayil, “Spray Coated Aluminum Oxide Thin Film For P-type Crystalline Silicon Surface Passivation,” pp. 8–11, 2015.

[16] C. N. Ajit and S. R. Jawalekar, “Thin Film Al_2O_3 Capacitors,” vol. 37, pp. 85–89, 1976.

[17] D. Perednis and L. J. Gauckler, “Thin Film Deposition Using Spray Pyrolysis,” pp. 103–111, 2005.

[18] P. S. Patil, “Versatility of Chemical Spray Pyrolysis Technique,” *Mater. Chem. Phys.*, vol. 59, pp. 185–198, 2010.

[19] M. Voigt and M. Sokolowski, “Electrical properties of thin rf sputtered aluminum oxide films,” pp. 1–5, 2004.

[20] F. Evangelisti, M. Stiefel, O. Guseva, R.P Nia, R. Hauert, E. Hack, L.P.H Jeurgens, F. Ambrosio, A. Pasquarello, P. Schmutz, C. Cancellieri, “Electrochimica Acta Electronic and structural characterization of barrier-type amorphous aluminium oxide,” *Electrochim. Acta*, vol. 224, pp. 503–516, 2017.

[21] T. Shirai, H. Watanabe, M. Fuji, and M. Takahashi, “Structural Properties and Surface Characteristics on Aluminum Oxide Powders.”

[22] I. Levin and D. Brandon, “Metastable Alumina Polymorphs : Crystal Structures and,” vol. 2012, no. 1998, pp. 1995–2012, 2012.

[23] P. Sciences and M. A. Aswad, “Residual Stress and Fracture in High Temperature Ceramics,” 2012.

[24] K. A. Matori, L. C. Wah, M. Hashim, and I. Ismail, “Phase Transformations of α -Alumina Made from Waste Aluminum via a Precipitation Technique,” vol. 2, pp. 16812–16821, 2012.

[25] V. P. Dhawale, V. Khobragade, and S. D. Kulkarni, “Synthesis and Characterization of Aluminium Oxide (Al_2O_3) Nanoparticles and its Application in Azodye Decolourisation,” vol. 2, no. 1, pp. 10–17, 2018.

[26] K. Ravindhranath and M. Ramamoorty, “Nano Aluminum Oxides As Adsorbents In Water Remediation Methods: A Review,” vol. 10, no. 3, pp. 716–722, 2017.

[27] N. Doskocz, K. Affek, and M. Z. Radziwiłł, “Effects of aluminium oxide nanoparticles on bacterial growth,” vol. 00019, pp. 1–7, 2017.

[28] P. Hassanpour, Y. Panahi, A. Ebrahimi-Kalan, A. Akbarzadeh, S. Davaran, A. N. Nasibova, R. Khalilov, T. Kavetskyy “Biomedical applications of aluminium oxide nanoparticles,” vol. 13, pp. 1227–1231, 2018.

[29] S. H. Tamboli, V. Puri, R. K. Puri, R. B. Patil, and M. Fan, “Comparative study of physical properties of vapor chopped and nonchopped Al 2 O 3 thin films,” *Mater. Res. Bull.*, vol. 46, no. 6, pp. 815–819, 2011.

[30] J. Saraie and S. Ngan, “Photo-CVD of Al 2 O 3 Thin Films,” *Jpn. J. Appl. Phys.*, vol. 29, no. Part 2, No. 10, pp. L1877–L1880, 1990.

[31] S. Robert, R. Rafati, A. Shari, and A. Cooper, “Application of aluminium oxide nanoparticles to enhance rheological and fi ltration properties of water based muds at HPHT conditions,” vol. 537, no. September 2017, pp. 361–371, 2018.

[32] N. N. Nikitenkov, O. V Vilkhivskaya, A. N. Nikitenkov, Y. I. Tyurin, V. S. Sypchenko, and I. A. Shulepov, “Interaction of Al 2 O 3 thin fi lms deposited on nanocrystalline titanium with hydrogen,” *Thin Solid Films*, vol. 591, pp. 169–173, 2015.

[33] R. A. Ismail, S. A. Zaidan, and R. M. Kadhim, “Preparation and characterization of aluminum oxide nanoparticles by laser ablation in liquid as passivating and anti-reflection coating for silicon photodiodes,” *Appl. Nanosci.*, vol. 7, no. 7, pp. 477–487, 2017.

[34] J. Kolodzey, E.A Chowdury, T.N Adam, G. Qui, I. Rau, J.O Olowolafe, J.S Suehle, Y. Chen, “Electrical Conduction and Dielectric Breakdown in Aluminum Oxide Insulators on Silicon,” vol. 47, no. 1, pp. 121–128, 2000.

[35] P. Zou, M. Yao, J. Chen, Y. Peng, and X. Yao, “Leakage current and dielectric breakdown in lanthanum doped amorphous aluminum oxide fi lms prepared by sol – gel,” vol. 42, pp. 4120–4125, 2016.

[36] C. W. Liang, T. C. Luoa, M. S. Fengb, H. C. Cheng, and D. Sue, “Characterization of anodic aluminum oxide film and its application to amorphous silicon thin film transistors,” vol. 43, pp. 166–172, 1996.

[37] K. Nomura, A. Takagi, T. Kamiya, H. Ohta, M. Hirano, H. Hosono, “Amorphous Oxide Semiconductors for High- Performance Flexible Thin-Film Transistors,” pp. 3–9, 2006.

[38] B. Urasinska-wojcik, N. Cocherel, R. Wilson, J. Burroughes, J. Opoku, M.L Turner, L.A Majewski, “1 Volt organic transistors with mixed self-assembled monolayer / Al 2 O 3 gate dielectrics,” vol. 26, pp. 20–24, 2015.

[39] K. S. Shamala, L. C. S. Murthy, M. C. Radhakrishna, and K. N. Rao, “Characterization of Al 2 O 3 thin films prepared by spray pyrolysis method for humidity sensor,” vol. 135, no. 2, pp. 552–557, 2007.

[40] C. Lin, D. Wuu, and J. Huang, “Surface & Coatings Technology Antireflection and passivation property of aluminium oxide thin fi lm on silicon nanowire by liquid phase deposition Concentration of AgNO (M),” *Surf. Coat. Technol.*, vol. 350, no. November 2017, pp. 1058–1064, 2018.

[41] M. Jacquet, “Characterization and adhesion study of thin alumina coatings sputtered on PET,” vol. 270, pp. 230–236, 1995.

[42] S. E. Potts, L. Schmalz, M. Fenker, B. Diaz, J. Swiatowska, J. Maurice, et. al, “Ultra-thin aluminium oxide films deposited by plasma- enhanced atomic layer deposition for corrosion protection Ultra-Thin Aluminium Oxide Films Deposited by Plasma-Enhanced Atomic Layer Deposition for,” no. 2011, pp. 4–11, 2019.

[43] J. G.-M. et Al, “Structural characteristics of Al 2 O 3 thin films prepared by spray pyrolysis Structural characteristics of Al 2 O 3 thin films prepared by spray pyrolysis,” vol. 13, no. 111, pp. 955–959, 2001.

[44] Y. Wu and K. Choy, “The microstructure of alumina coatings prepared by aerosol assisted spray deposition,” vol. 181, pp. 436–440, 2004.

[45] T. Xiufeng, A. Physics, S. Processing, and M. Science, “Effects of the Annealing Heating Rate on Sputtered Aluminum Oxide Films,” vol. 32, no. 1, pp. 94–99.

[46] W. Xia, G. Xia, G. Tu, X. Dong, S. Wang, and R. Liu, “Sol-gel processed high- k aluminum oxide dielectric fi lms for fully solution- processed low-voltage thin- fi lm transistors,” *Ceram. Int.*, vol. 44, no. 8, pp. 9125–9131, 2018.

[47] T. B. Tai, L. Cao, F. Mattelaer, G. Rampelberg, F.S.M Hashemi, J. Dendooven, J.R van Ommen,

C. Detavernier, M.F Reyniers, “Atomic Layer Deposition of Al2O3 Using Aluminum Triisopropoxide (ATIP): A Combined Experimental and Theoretical Study,” *J. Phys. Chem. C*, vol. 123, no. 1, pp. 485–494, 2019.

[48] J. M. Andersson, *Controlling the Formation and Stability of Alumina Phases*, no. 987. 2005.

[49] R. D. Gould, S. Kasap, and A. K. Ray, *Handbook of Electronic and Photonic Materials-Thin Films*. 2017.

[50] A. et al. Jilani, “Advance Deposition Techniques for Thin Film and Coating,” no. March, 2017.

[51] J. E. Crowell, “Chemical methods of thin film deposition: Chemical vapor deposition, atomic layer deposition, and related technologies,” *J. Vac. Sci. Technol. A Vacuum, Surfaces, Film.*, vol. 21, no. 5, pp. S88–S95, 2003.

[52] W. Ban, S. Kwon, J. Nam, J. Yang, S. Jang, and D. Jung, “Al 2 O 3 thin fi lms prepared by plasma-enhanced chemical vapor deposition of dimethylaluminum isopropoxide,” vol. 641, pp. 47–52, 2017.

[53] N. Koslowski, S. Sanctis, and J. Schneider, “a thin film transistor device of amorphous aluminum oxide Al x O y using a molecular based precursor route †,” pp. 33–36, 2019.

[54] J. Huh, J. Park, J. Lee, S. Lee, J. Lee, K-H Lim, Y.S Kim, “Journal of Industrial and Engineering Chemistry Effects of process variables on aqueous-based AlO x insulators for high-performance solution-processed oxide thin- fi lm transistors,” vol. 68, pp. 117–123, 2018.

[55] J. H. Jun, H. J. Kim, and D. J. Choi, “Processing Research Effect of the hydration on the properties of an aluminum oxide film,” vol. 9, no. 1, pp. 75–78, 2008.

[56] R. Rammula, L. Aarik, A. Kasikov, J. Kozlova, and T. Kahro, “Atomic layer deposition of aluminum oxide films on graphene Atomic layer deposition of aluminum oxide films on graphene,” pp. 0–4, 2013.

[57] H. Garcia, H. Castan, and S. Duenas, “Advanced electrical characterization of atomic layer deposited Al203 MIS-based structures ~ : ~ I : ==,” pp. 1–4, 2017.

[58] Y. Shao, X. Wu, M. N. Zhang, W. J. Liu, and S. J. Ding, “High-Performance a-InGaZnO Thin-Film Transistors with Extremely Low Thermal Budget by Using a Hydrogen-Rich Al 2 O 3 Dielectric,” *Nanoscale Res. Lett.*, vol. 14, pp. 2–7, 2019.

[59] S. H. Tamboli, V. Puri, R. K. Puri, R. B. Patil, and M. Fan, “Comparative study of physical properties of vapor chopped and nonchopped Al 2 O 3 thin films,” vol. 46, pp. 815–819, 2011.

[60] J. Schmidt, A. Merkle, and B. Hoex, “Surface Passivation of High-efficiency Silicon Solar Cells,” no. December 2017, 2008.

[61] L. A. Dobrzański, M. Szindler, A. Drygała, and M. M. Szindler, “Silicon solar cells with Al2O3 antireflection coating,” *Cent. Eur. J. Phys.*, vol. 12, no. 9, pp. 666–670, 2014.

[62] A. K. Singh, R. G. Hennig, A. V. Davydov, F. Tavazza, “Al2O3 as a suitable substrate and a dielectric layer for n-layer MoS2 Al 2 O 3 as a suitable substrate and a dielectric layer for n -layer MoS 2,” vol. 053106, no. 2015, 2017.

[63] S. Ramesh and S. Dutta, “Identification of current transport mechanism in Al 2 O 3 thin films for memory applications Si Substrate,” 2014.

[64] M. Eslamian, “Inorganic and Organic Solution-Processed Thin Film Devices,” *Nano-Micro Lett.*, 2017.

[65] F. F. Vidor, T. Meyers, and U. Hilleringmann, “Flexible Electronics: Integration Processes for Organic and Inorganic Semiconductor-Based Thin-Film Transistors,” pp. 480–506, 2015.

[66] G. Horowitz, “Organic thin film transistors: From theory to real devices,” *J. Mater. Res.*, vol. 19, no. 7, pp. 1946–1962, 2004.

[67] Z. A. Lamport, H. F. Haneef, S. Anand, M. Waldrip, and O. D. Jurchescu, “Tutorial: Organic field-effect transistors: Materials, structure and operation,” *J. Appl. Phys.*, vol. 124, no. 7, 2018.

[68] C. Falcony, M. A. Aguilar-Frutis, and M. García-Hipólito, “Spray pyrolysis technique; High-K dielectric films and luminescent materials: A review,” *Micromachines*, vol. 9, no. 8, pp. 1–33, 2018.

[69] B. W. Mwakikunga, “Progress in Ultrasonic Spray Pyrolysis for Condensed Matter Sciences Developed From Ultrasonic Nebulization Theories Since Michael Faraday Progress in Ultrasonic Spray Pyrolysis for Condensed Matter Sciences Developed From Ultrasonic,” vol. 8436, no. October 2017, 2014.

[70] J. B. Mooney and S. B. Radding, “Spray Pyrolysis Processing,” *Annu. Rev. Mater. Sci.*, vol. 12, no. 1, pp. 81–101, 1982.

[71] L. Filipovic, S. Selberherr, G. C. Mutinati, E. Brunet, S. Steinhauer, A. Kock, J. Teva, J. Kraft, J. Siegert, F. Schrank, “Modeling Spray Pyrolysis Deposition,” *Proc. World Congr. Eng.*, vol. II, pp. 6–11, 2013.

[72] G. L. Messing, S.-C. Zhang, and G. V Jayanthi, “Ceramic Powder Synthesis,” *J.Am.Ceram.Soc*, vol. 11, no. 76, pp. 2707–26, 1993.

[73] S. C. Tsai, Y. L. Song, C. C. Yang, W. Y Chiu, H. M. Lin, “Ultrasonic spray pyrolysis for nanoparticles synthesis,” *J. Mater. Sci.*, vol. 9, pp. 3647–3657, 2004.

[74] M. S. Tomar and F. J. Garcia, “Spray pyrolysis in solar cells and gas sensors,” *Prog. Cryst. Growth Charact.*, vol. 4, no. 3, pp. 221–248, 1981.

[75] M. F. García-Sánchez, J. Pena, A. Oritz, G. Santana, J. Fandino, M. Bizarro, F. Cruz - Guandarilla, J. C. Alonso, “Nanostructured YSZ thin films for solid oxide fuel cells deposited by ultrasonic spray pyrolysis,” *Solid State Ionics*, vol. 179, no. 7–8, pp. 243–249, 2008.

[76] E. Kärber, A. Katerski, I. O. Acik, A. Mere, V. Mikli, and M. Krunks, “Sb 2 S 3 grown by ultrasonic spray pyrolysis and its application in a hybrid solar cell,” 2016.

[77] I. Dundar, M. Krichevskaya, A. Katerski, I. O. Acik, and I. Dundar, “TiO 2 thin films by ultrasonic spray pyrolysis as photocatalytic material for air purification,” 2019.

[78] S. Polivtseva, I. O. Acik, A. Katerski, A. Mere, V. Mikli, and M. Krunks, “Spray pyrolysis deposition of Sn x S y thin films,” vol. 60, no. May, pp. 156–165, 2014.

[79] A. T. Oluwabi, I. O. Acik, A. Katerski, A. Mere, and M. Krunks, *Structural and electrical characterisation of high-k ZrO2 thin films deposited by chemical spray pyrolysis method.* Elsevier B.V, 2018.

[80] A. A. Dronov, D. A. Dronova, E. P. Kirilenko, I. M. Terashkevich, and S. A. Gavrilov, “Studying

Composition of Al 2 O 3 Thin Films Deposited by Atomic Layer Deposition (ALD) and Electron-Beam Evaporation (EBE) upon Rapid Thermal Processing," vol. 12, no. 4, pp. 428–433, 2017.

[81] and S. S. Y. Koda, H. Sugita, T. Suwa, R. Kuroda, T. Goto, A. Teramoto, "Low Leakage Current Al 2 O 3 Metal-Insulator-Metal Capacitors Formed by Atomic Layer Deposition at Optimized Process Temperature and O 2 Post Deposition Annealing Y. Koda," *E C S Trans. Electrochem. Soc.*, vol. 72, no. 4, pp. 91–100, 2016.

[82] B. L. Yang, P. T. Lai, and H. Wong, "Conduction mechanisms in MOS gate dielectric films," vol. 44, pp. 709–718, 2004.

[83] J. Lee, S. S. Kim, S. Im, J. Lee, S. S. Kim, and S. Im, "Electrical properties of aluminum oxide films deposited on indium-tin-oxide glasses Electrical properties of aluminum oxide films deposited on indium-tin-oxide glasses," vol. 953, no. 2003, pp. 2–6, 2015.

CYSENI 2019, May 23-24, Kaunas, Lithuania
ISSN 1822-7554, www.cyseni.com

CHARACTERISATION OF ALUMINUM OXIDE THIN FILMS DEPOSITED BY SPRAY PYROLYSIS

K.D. Omotosho, A.T. Oluwabi, I. Oja Acik, Arvo Mere, Malle Krunks
Laboratory of Thin Film Chemical Technologies
Department of Materials and Environmental Technology
Tallinn University of Technology
Ehitajate tee 5, EE-19086 Tallinn, Estonia.
Phone: +372 58781560
Email: komoto@ttu.ee

ABSTRACT

Aluminum Oxide (AlO_x) is a high-k semiconductor material with excellent optical and electrical properties, and it has been successfully used in different applications most especially as a gate insulator for thin film transistors. For the purpose of this work, an ultrasonic spray pyrolysis (USP) method was adopted. To the best of our knowledge, limited work has been done on USP deposition of AlO_x thin films. Aluminum acetylacetonate salt $Al(acac)_3$ was used as the AlO_x precursor salt. 0.05 M concentration of AlO_x precursor was prepared by dissolving Aluminum acetylacetonate in methanol, the solution was sprayed onto heated silicon wafer and quartz substrates at temperatures of 350, 450, and 550 ^oC. As-deposited films on quartz substrates were annealed at 500, 800, and 1000 ^oC for 1 hour. The microstructural, morphological and electrical properties of the films were investigated. The X-ray diffraction (XRD) studies revealed that both as-deposited and annealed AlO_x thin films were amorphous. Scanning electron microscope (SEM) images revealed that the AlO_x films were smooth, uniform, and well compacted with the absence of grain boundaries. Electrical properties of the as-deposited AlO_x thin film was accessed by constructing capacitor in a metal-insulator-structure (MIS). As revealed by the current – voltage characterization, the resistivity of the as-deposited film increases with deposition temperature from $3.07x10^4$ Ωcm (in 350^{o}C as-deposited films) to $1.57x10^5$ Ωcm (in 450^{o}C as-deposited film). The films have a high dielectric constant in the range of 7.4 – 5.6. Based on this result, USP as-deposited AlO_x film shows promising properties suitable for use in transistor application.

Keywords: Aluminum oxide, Spray pyrolysis, Dielectric, Thin films transistor, Current-voltage

1. INTRODUCTION

Aluminum Oxide (AlO_x) is considered an outstanding material for application in microelectronics, optoelectronics, sensors, water repellent coating, protective coating, gate dielectric in thin film transistors (TFTs), biomedicals and sensing layer due to the following properties: excellent dielectric constant; wide band gap; low-leakage current densities; good adhesion to glass substrate; chemical inertness; high thermal conductivity; high refractive index; and mechanical strength [1]–[5].

Amorphous AlO_x is considered as a suitable gate dielectric in TFTs to avoid leakage current through crystalline grain boundaries [2]. In order to reduce the size of metal oxide semiconductor (MOS) transistors below 50 nm for next generation electronic devices, amorphous materials that are novel with high dielectric constant, high breakdown voltage, low leakage and low interface trap density values are needed [3]. AlO_x has a band gap and dielectric constant of 9.9 eV and 10 respectively compared to SiO_2 with band gap of 9 eV and dielectric constant of 3.9 [3].

M. Aguilar Frutis et al. [5] have investigated the effect of adding water to the AlO_x spray precursor solution on the optical properties of the film formed. The thin film from the addition of water mist showed the highest refractive index (~ 1.66), and lower content of -OH and water related bonds, while the AlO_x thin film without addition of water mist has low value of refractive index with presence of water related impurities and -OH bonds.

It was reported by J. Jun et al. [6] that hydration improves the properties of AlO_x films. They discovered that increase in dipping time of AlO_x films in deionized water increases the dielectric constant from 7.8 to 11.5 with no significant increase in leakage current. This effect is due to the structural change of the film surface from aluminum oxide to pseudo-boehmite after reaction with water. J. Kolodzey et al. [7] also confirmed the effect of difference in oxidation conditions, sublayer composition and structure in the variation of current-density characteristics.

With respect to the effect of atmosphere in which dielectric measurement is carried out, N. Koslowski et al. [8] revealed that dielectric measurements done in ambient temperature increases the capacitance significantly and affect parasitic resistance due to water molecules from the atmosphere adsorbed on the film surface. It was established that AlO_x films deposited by spin coating method at high humid conditions improves the electrical properties of the film by producing a smooth film surface, very low leakage current and higher breakdown voltage. At low humid conditions, spherulite structure in form of cracks are formed on the surface of the films leading to unfavorable dielectric properties [9]. WenWen et al. in their recent study reported that increasing annealing temperature of AlO_x film decreases the leakage current density of the film and vice versa. The reduced leakage current was attributed to the decrease in oxygen defect as Al-O bonding forms, and the large leakage current was due to the presence of hydroxyl group and residual organics which form the conduction paths. They also recorded a large dielectric value of 13.8 for low temperature annealed AlO_x film, which was ascribed to the large amount of hydroxyl group revealed by the XPS result [10].

According to our review, AlO_x thin films prepared by other deposition methods such as pulsed laser deposition (PLD) [3], chemical vapor deposition (CVD) [11], [12], plasma enhanced chemical vapor deposition (PECVD) [13], and plasma enhanced atomic layer deposition (PEALD) [14], [15] have been studied extensively, however, only limited research could be found on AlO_x thin films deposited by chemical spray pyrolysis. Of all these methods, the spray pyrolysis is considered to be optimal due to its simplicity and low-cost as it does not require a vacuum [16], its ease in doping, it doesn't require a high quality target/substrate, it also offers an easy method of adjusting the deposition rate and film thickness by altering spray parameters [17].

In this paper, we focus on the deposition of AlO_x thin film by the USP method with the aim of studying the influence of varying deposition temperature and

annealing temperature on the film's structural, morphological and electrical properties for its application as a dielectric layer in thin film transistor technology.

2. METHODOLOGY

AlO_x films were deposited onto a preheated substrate of silicon and quartz with dimension 2 cm by 1 cm by ultrasonic spray pyrolysis (USP) technique. The substrates were cleaned in methanol, ethanol and deionized water in ultrasonic bath for 5 minutes each at 60 ºC. The precursor solution of 250 ml volume with 0.05 M concentration were prepared by dissolving 4.05 g aluminum acetylacetonate ($Al(C_5H_7O_2)_3$) powder in methanol (CH_3OH) and the solution was stirred for 15 mins with a magnetic stirrer at room temperature to ensure homogeneity. The solution was atomized by an ultrasonic generator of 1.7 MHz frequency, and the generated aerosol was transported directly to the heated substrates using air as carrier. Films were deposited by spraying 50 ml solution of AlO_x with the same molar concentration at various substrate temperatures, (Ts) of 350 ºC, 450 ºC and 550 ºC in air. The carrier gas flow rate and director gas flow rate for spraying the solution were 3 L/min and 1 L/min respectively. For the deposition, spray parameters were set as 3 steps, 10 cycles. Structural studies were carried out on the quartz substrate, while electrical studies were carried out on the silicon substrate.

The as-deposited AlO_x films on quartz and silicon substrates were annealed in air at temperatures of 500 ºC, 800 ºC, and 1000 ºC for 1 hour using a Nabertherm L5/11/06D furnace. X-Ray diffraction (XRD) measurement was carried out with the RIKAGU ULTIMA IV diffractometer with Cu Kα radiation ($\gamma = 1.5406$ Å, 40 kV, 40 mA) using silicon strip detector D/tex Ultra. Sample measurement were taken in the 2Θ range from 20-60 degree with a step of 0.02º and scanning speed of 5 º/min.

The surface morphology, cross-sections were investigated with the aid of Zeiss HR FESEM Ultra 55 high-resolution scanning electron microscopy (SEM). The accelerated voltage for SEM measurement was 4.0 kV.

A metal-oxide semiconductor (MIS) with structure Al/AlOx/Si-C was fabricated for the purpose of electrical measurement by evaporating Aluminum electrode contact on the surface of the films with the help of Quorum K975X vacuum evaporator. A mask with uniform area 1.7 mm^2 was used to cover the films before deposition. Graphite paste was applied on the back side of the device to improve ohmic conductivity, and measurement was carried out through both the graphite and Al. The I-V and impedance measurements were carried out using the AUTOLAB PGSTAT 30 equipment.

3. RESULTS AND DISCUSSIONS

3.1. Surface Morphology

Figure 1 shows the surface morphology and cross-section views of AlO_x films grown at 350 ºC, 450 ºC and 550 ºC on quartz substrate. The surface of the films deposited were homogenous, well compacted, and smooth, with the presence of some random particles of about 100 nm size. According to Alexey et al. AlO_x thin film deposited by atomic layer deposition method also show smooth surface [18].

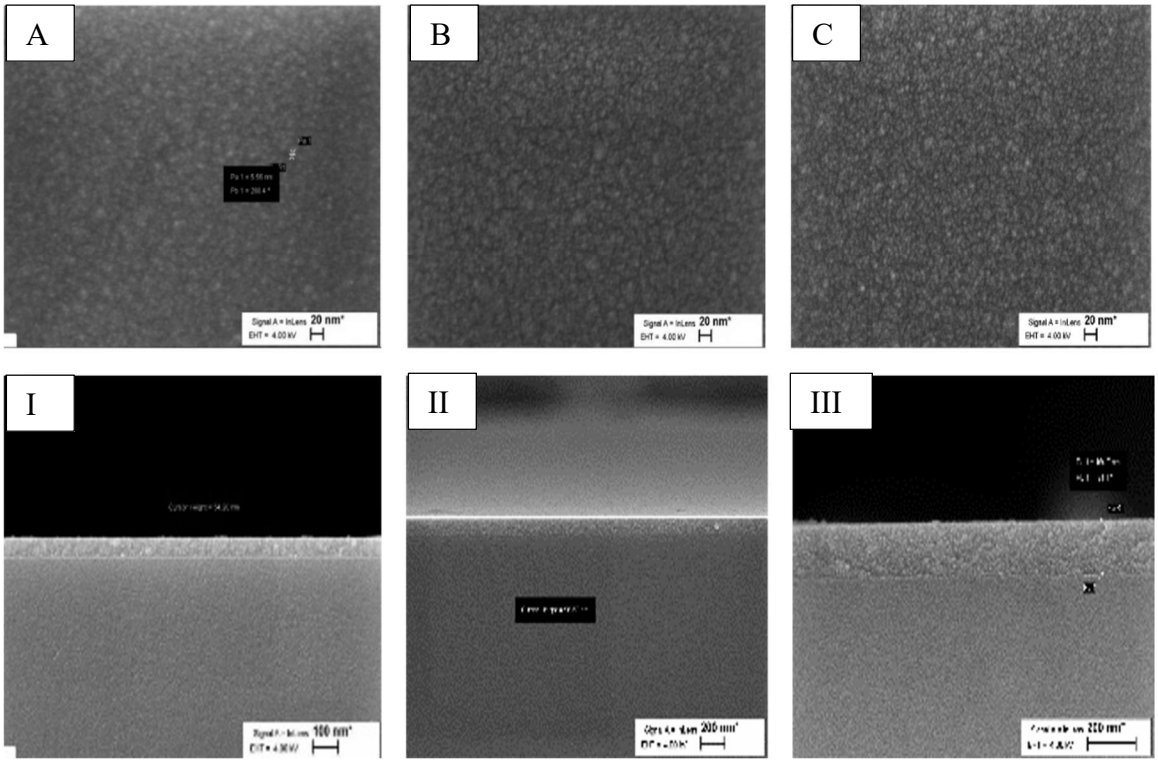

Fig. 1. SEM images with cross-section of 0.05 M concentration of AlO_x films as-deposited at 350 ºC (A-I), 450 ºC (B-II), and 550 ºC (C-III)

The thicknesses of the films were estimated from the cross-sectional images shown in Fig. 1. (1-III). The obtained results revealed that the thicknesses of the films increase with increase in deposition temperature. The thickness of the film as-deposited at 350 ºC is 54 nm, while the thickness of films as-deposited at 450 ºC and 550 ºC are 96 nm and 159 nm respectively.

3.2. Structural Studies

The X-ray diffractogram of AlO_x films as-deposited at 350 ºC and 450 ºC followed by annealing at 1000 ºC on quartz substrates is shown in Figure 2. The X-ray diffractogram of the as-deposited AlO_x films and annealed AlO_x films at 500, and 800 ºC show a similar pattern to the film annealed at 1000 ºC below. No peaks are observed on the diffractogram, which proves that all the samples were amorphous with no degree of crystallinity in the films. Our result also corresponds with XRD measurements of AlO_x films in previous literatures that no sharp peak was observed for AlO_x film annealed until annealing temperature of 1000 ºC [12][10][8].

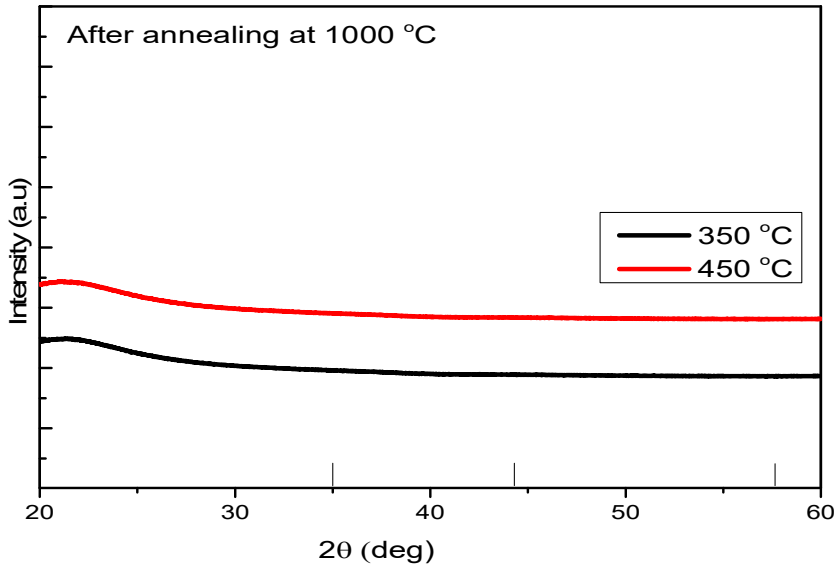

Fig. 2. X-ray diffractogram of AlOx thin films as-deposited at 350 °C, 450 °C, and annealed at 1000 °C

3.3. Electrical Studies

3.3.1. Current-voltage characterisation

Electrical properties of the AlO_x films were characterized by constructing a capacitor of $Al/AlO_x/Si$ structure. Figure 3 shows the leakage current density in the forward bias and reverse bias regime (-2 V to +2 V). The current density at -1.0 V was estimated to be 9.5×10^{-8} A/cm^2, 1.5×10^{-5} A/cm^2, and 1.6×10^{-6} A/cm^2 for AlO_x as-deposited at 350 °C, 450 °C, and 550 °C respectively. J. Jun et al. [6] reported a leakage current of 3.8×10^{-4} A/cm^2 for as-deposited AlO_x thin film by metal organic chemical vapor deposition. Y. Koda et al. [20] also reported leakage current density of 3.6×10^{-10} A/cm^2 for as-deposited AlO_x films. Our leakage current values are close to the values reported in previous literatures.

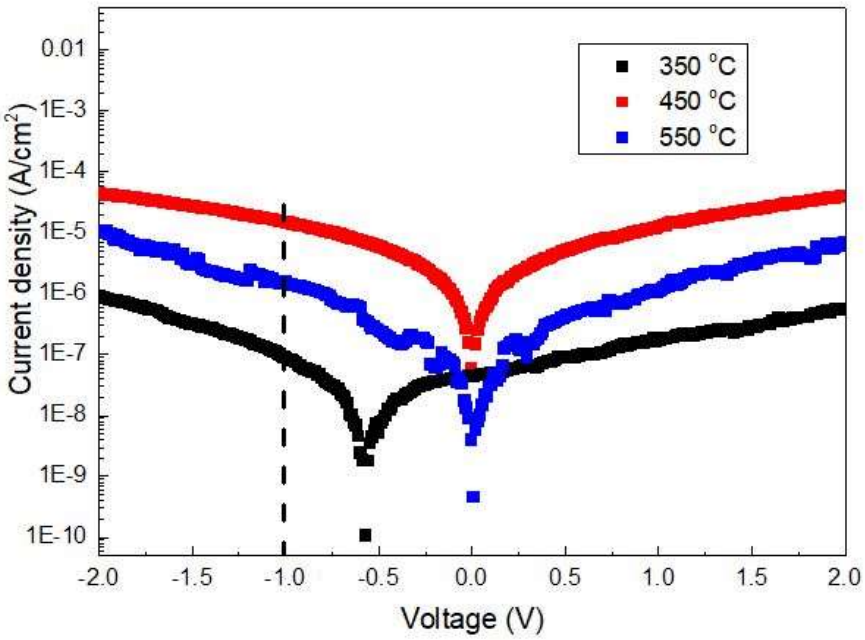

Fig. 3. Leakage current density for AlO_x thin films as-deposited at 350, 450, and 550 °C

It can be seen from the result that AlO_x thin film as-deposited at 350 °C has a very small leakage current. This small leakage current could be attributed to a smooth and compact surface of the sample due to the absence of grain boundaries which may act as leakage channel resulting in a large leakage current. Presence of Al-O bonding on the film surface as a result of film condensation at higher deposition temperature also decreases the leakage current of dielectric layer [10]. It also shows that 350 °C deposition temperature could presumably be sufficient to achieve a good dielectric with low leakage current by using USP technique.

The electrical resistivity ρ (Ω cm) of the AlO_x dielectric film was estimated from resistance R (Ω) using equation below.

$$\rho = R \frac{A}{L} \qquad (1)$$

Where L is the thickness of the film, A is the contact area, and R is the resistance. The values for electrical conductivity was calculated by taking inverse of resistivity. The resistivity values for the as-deposited AlO_x thin film at 350 °C, 450 °C and 550 °C are estimated to be 3.1×10^4 Ωcm, 1.6×10^5 Ωcm, and 3.9×10^1 Ωcm respectively. It can be observed that AlO_x thin films as-deposited at 450 °C has a large electrical resistivity among all the samples which could be as a result of its small thickness. The resistivity of the films increases with increasing deposition temperature from 350 °C to 450 °C.

3.3.2. Dielectric-characterisation

Capacitance value was extracted from the impedance and both the mean area capacitance and mean dielectric constants were estimated at different contacts for all working devices at different frequencies. The capacitance-frequency box plot for as-deposited AlO_x thin films on silicon substrates is shown in Figure 4. This plot shows the range of calculated area capacitance values for all the samples at different frequencies of 1 kHz, 10 kHz, and 100 kHz. It is seen that capacitance of AlO_x film as-deposited at 350 ºC decreases with increase in the frequency. This phenomenon of reduced capacitance at high frequency is linked to the presence of trap states in dielectric films which prevents the film from acquiring enough speed needed to match higher frequencies [21]. On the other hand, capacitance values for AlO_x as-deposited at 450 ºC and 550 ºC were relatively stable across the frequency range. The variation in capacitance could be attributed to the presence of hydroxyl groups in the AlO_x films. Large amount of hydroxyl groups could lead to significant decrease in capacitance and vice versa [10]. The Capacitance (C) of the samples was estimated from equation below.

$$C = \frac{1}{2\pi f\ ''} \qquad (2)$$

Where f is the frequency, Z" is the imaginary impedance, π is a constant = 3.1415.

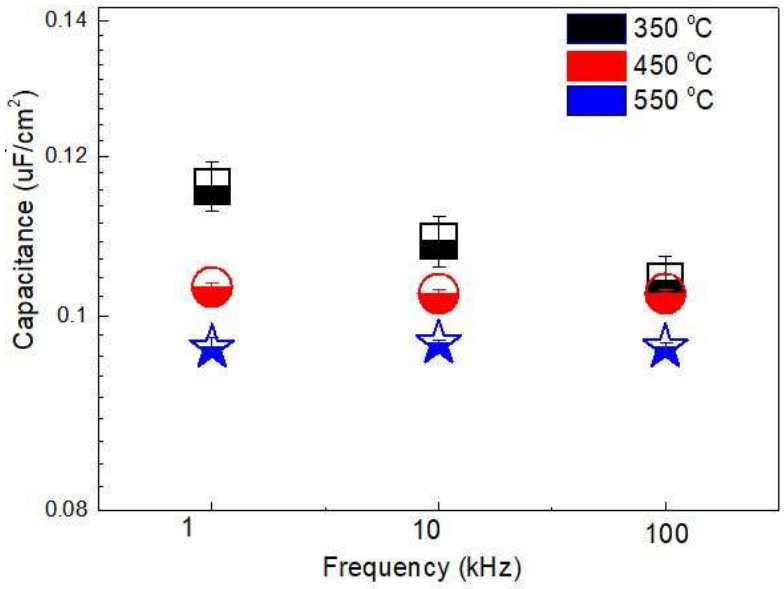

Fig. 4. Capacitance-Frequency plot for the AlO_x as-deposited on Si at 350, 450 and 550 ºC

AlO_x film as-deposited at 350 ºC, 450 ºC, and 550 ºC at 1 kHz exhibited mean capacitance values of 116 nF/cm^2, 57 nF/cm^2, and 36 nF/cm^2 respectively. Area capacitance reported by Wenwen et al. [10] for annealed AlO_x films were in the

range of 72.2 -120.6 nF/cm^2. It was also observed that the capacitance values decrease with increase in deposition temperature.

Figure 5 shows the dependence of dielectric constant on frequency for as-deposited AlO_x samples on silicon substrates. It was found that the sample as-deposited at 350 ^oC has a large dielectric constant value of approximately 7.4 at 1 kHz. Reported values of dielectric constant for as-deposited AlO_x films are in the range of 7-10 [22][23]. At higher frequency dispersion, mean dielectric constant for sample as-deposited at 350 ^oC is almost equal to that of the sample as-deposited at 550 ^oC.

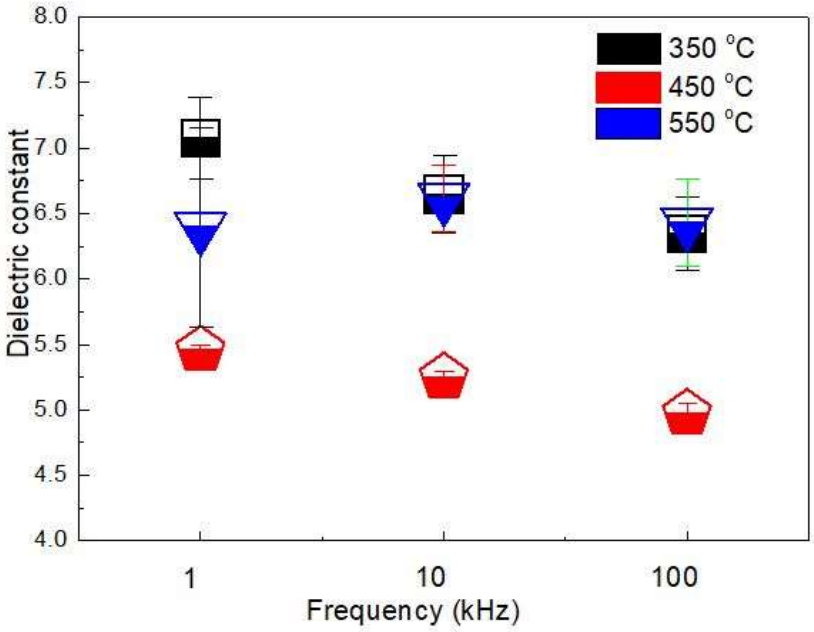

Fig. 5. Dielectric-Frequency plot for the AlO_x as-deposited on Si at 350, 450 and 550 ^oC

Dielectric constant, k was determined using the following equation:

$$C = \frac{\varepsilon_o k A}{d} \quad (3)$$

Where C is the capacitance, ε_o is permittivity of free space, k is the dielectric constant, A is the contact area, d is the AlO_x film thickness.

Table 1. Summary of the dielectric constant values and area capacitance at 1kHz for all the as-deposited samples.

As-deposited Samples (°C)	Area (cm^2)	Dielectric constant @ 1kHz	Area Capacitance (nF/cm^2) @1kHz
350	0.017	7.4	116
450	0.017	5.6	57
550	0.017	6.5	36

4. CONCLUSIONS

The ultrasonic spray pyrolysis method was successfully used to deposit smooth and homogenous AlO_x thin films of 0.05 M concentration at deposition temperatures of 350 °C, 450 °C and 550 °C on silicon and quartz substrates. The SEM images reveal that the AlO_x samples as-deposited were smooth, homogenous and compact. Film thickness increases with deposition temperature. XRD data shows that the as-deposited films were amorphous. Further annealing at 500 °C, 800 °C and 1000 °C shows amorphous films with no diffraction peak observed. The films were highly resistive with high dielectric constant in the range of 7.4-5.6 depending on the deposition temperature (350 °C - 550 °C). The results indicated that AlO_x thin films deposited by ultrasonic spray pyrolysis is suitable as a gate dielectric layer in thin film transistor application.

5. ACKNOWLEDGEMENTS

The authors acknowledge V. Mikli for SEM measurements. This study was financially supported by the Estonian Ministry of Education and Research, project IUT19-4, and by the European Union through the European Regional Development Fund, project TK141 ‘Advanced materials and high technology devices for energy recuperation systems’.

REFERENCES

1. NILAI, P., SEMBILAN, N. “International Journal of Chemical Preparation of Nanocrystalline Aluminum Oxide Thin Films : A Review,” vol. 15, no. 2, pp. 1–8, 2018.

2. CUI, J. *et al.* “Aluminum Oxide Thin Films from Aqueous Solutions: Insights from Solid-State NMR and Dielectric Response,” *Chem. Mater.*, vol.

30, no. 21, pp. 7456–7463, 2018.

3. KATIYAR, P., JIN, C., and NARAYAN, R.J. “Electrical properties of amorphous aluminum oxide thin films,” vol. 53, pp. 2617–2622, 2005.

4. GUZMAN-MENDOZA, J. et al. “Structural characteristics of Al 2 O 3 thin films prepared by spray pyrolysis Structural characteristics of Al 2 O 3 thin films prepared by spray pyrolysis,” vol. 13, no. 111, pp. 955–959, 2001.

5. AGUILAR-FRUTIS, M., GARCIA, M., FALCONY, C., PLESCH, G., and JIMENEZ-SANDOVAL, S. “A study of the dielectric characteristics of aluminum oxide thin films deposited by spray pyrolysis from Al Ž acac . 3,” pp. 200–206, 2001.

6. JUN, J. H., KIM, H. J., and CHOI, D. J. “Processing Research Effect of the hydration on the properties of an aluminum oxide film,” vol. 9, no. 1, pp. 75–78, 2008.

7. KOLODZEY, J. *et al.* “Electrical Conduction and Dielectric Breakdown in Aluminum Oxide Insulators on Silicon,” vol. 47, no. 1, pp. 121–128, 2000.

8. KOSLOWSKI, N., SANCTIS, S., and SCHNEIDER, J. “a thin film transistor device of amorphous aluminum oxide Al x O y using a molecular based precursor route †,” pp. 33–36, 2019.

9. HUH, J. *et al.* “Journal of Industrial and Engineering Chemistry Effects of process variables on aqueous-based AlO x insulators for high-performance solution-processed oxide thin- fi lm transistors,” vol. 68, pp. 117–123, 2018.

10. XIA, W., XIA, G., TU, G., DONG, X., WANG, S., and LIU, R. “Sol-gel processed high- k aluminum oxide dielectric fi lms for fully solution-processed low-voltage thin- fi lm transistors,” *Ceram. Int.*, vol. 44, no. 8, pp. 9125–9131, 2018.

11. MARUYAMA, T. and ARAI, S. “Aluminum oxide thin films prepared by chemical vapor deposition from aluminum acetylacetonate Aluminum oxide thin films prepared from aluminum acetylacetonate by chemical vapor deposition,” vol. 322, no. 1992, pp. 1998–2000, 2013.

12. KIYOTO Lida. “Physical and Chemical Properties of Aluminum Oxide Film Deposited by Iida_1972_Jpn._J._Appl._Phys._11_840.pdf.” Japanese Journal of Applied Physics, 1972.

13. KALAIVANI, S. and KOTTANTHARAYIL, A. “Spray Coated Aluminum Oxide Thin Film For P-type Crystalline Silicon Surface Passivation,” pp. 8–11, 2015.

14. LALE, A., SCHEID, E., CRISTIANO, F., DATAS, L., and REIG, B. “Study of aluminium oxide thin fi lms deposited by plasma-enhanced atomic layer deposition from tri-methyl-aluminium and dioxygen precursors : Investigation of interfacial and structural properties,” vol. 666, no. December

2017, pp. 20–27, 2018. [15] H. Y. Li, Y. F. Liu, Y. Duan, Y. Q. Yang, and Y. N. Lu, “Method for aluminum oxide thin films prepared through low temperature atomic layer deposition for encapsulating organic electroluminescent devices,” *Materials (Basel).*, vol. 8, no. 2, pp. 600–610, 2015.

15. LI, H. Y., LIU, Y. F., DUAN, Y., YANG, Y. Q., and LU, Y. N. “Method for aluminum oxide thin films prepared through low temperature atomic layer deposition for encapsulating organic electroluminescent devices,” *Materials (Basel).*, vol. 8, no. 2, pp. 600–610, 2015.

16. FALCONY, C., AGUILAR-FRUTIS, M. A., and GARCIA-HIPOLITO, M. “Spray pyrolysis technique; High-K dielectric films and luminescent materials: A review,” *Micromachines*, vol. 9, no. 8, pp. 1–33, 2018.

17. PATIL, P. S. “Versatility of Chemical Spray Pyrolysis Technique,” *Mater. Chem. Phys.*, vol. 59, pp. 185–198, 2010.

18. DRONOV, A. A, DRONOVA, D. A., KIRILENKO, E. P., TERASHKEVICH, I. M., and GAVRILOV, S. A. “Studying Composition of Al 2 O 3 Thin Films Deposited by Atomic Layer Deposition (ALD) and Electron-Beam Evaporation (EBE) upon Rapid Thermal Processing,” vol. 12, no. 4, pp. 428–433, 2017.

19. RAVINDHRANATH, K., RAMAMOORTY, M., “nano aluminum oxides as adsorbents in water remediation methods : a review,” vol. 10, no. 3, pp. 716–722, 2017.

20. KODA, Y., SUGITA, H., SUWA, T., KURODA, R., GOTO, T., TERAMOTO, A., SUGAWA, S. “Low Leakage Current Al 2 O 3 Metal-Insulator-Metal Capacitors Formed by Atomic Layer Deposition at Optimized Process Temperature and O 2 Post Deposition Annealing Y. Koda,” *E C S Trans. Electrochem. Soc.*, vol. 72, no. 4, pp. 91–100, 2016.

21. KIM, J., CHOI, S., KIM, M., HA, T., and KIM, Y. “Strontium doping e ff ects on the characteristics of solution-processed aluminum oxide dielectric layer and its application to low-voltage-operated indium-gallium-zinc-oxide thin- fi lm transistors,” *Ceram. Int.*, vol. 43, no. 16, pp. 13576–13580, 2017.

22. LEE, J., KIM, S. S., IM, S., LEE, J., KIM, S. S., and IM, S. “Electrical properties of aluminum oxide films deposited on indium-tin-oxide glasses Electrical properties of aluminum oxide films deposited on indium-tin-oxide glasses,” vol. 953, no. 2003, pp. 2–6, 2015.

23. VOIGT, M., SOKOLOWSKI, M. “Electrical properties of thin rf sputtered aluminum oxide films,” pp. 1–5, 2004.